Early 2022 breakthrough infection sera from India target the conserved cryptic class 5 epitope to counteract immune escape by SARS-CoV-2 variants

Indrani Das Jana[1], Kawkab Kanjo[2], Subhanita Roy[1], Munmun Bhasin[2], Shatarupa Bhattacharya[5], Indranath Banerjee[3], Subhasis Jana[6], Arjun Chatterjee[7], Alok Chakraborty[8], Suman Chakraborty[4], Budhaditya Mukherjee[5], Raghavan Varadarajan[2*], Arindam Mondal[1*]

[1]Department of Bioscience and Biotechnology, Indian Institute of Technology Kharagpur, Kharagpur-721302, India
[2]Molecular Biophysics Unit (MBU), Indian Institute of Science, Bengaluru-560012, India
[3]B.C. Roy Technology Hospital, Indian Institute of Technology Kharagpur, Kharagpur-721302, India
[4]Department of Mechanical Engineering, Indian Institute of Technology Kharagpur, Kharagpur-721302, India
[5]School of Medical Science and Technology, Indian Institute of Technology Kharagpur, Kharagpur-721302, India
[6]Purba Medinipur District Hospital, Tamluk-721636, India
[7]Institute of Neuroscience, Kolkata-700017
[8]ICMR-National Institute of Cholera and Enteric Diseases, Kolkata-700010, India

Correspondence*: varadar@iisc.ac.in (R.V.), arindam.mondal@iitkgp.ac.in (A.M.)

Abstract:

During the COVID-19 pandemic, the vast majority of epitope mapping studies have focused on sera from mRNA-vaccinated populations from high-income countries. In contrast, here we report an analysis of 164 serum samples isolated from breakthrough infection patients in India during early 2022 who received two doses of the ChAdOx viral vector vaccine. Sera were screened for neutralization breadth against wildtype, Kappa, Delta, and Omicron BA.1 viruses. Three sera with the highest neutralization breadth and potency were selected for epitope mapping using charged scanning mutagenesis coupled to yeast surface display and Next Generation Sequencing. All of these sera primarily targeted the recently identified class 5 cryptic epitope along with the class 1 and class 4 epitopes, targeted to a lesser extent. The class 5 epitope is completely conserved across all SARS-CoV-2 variants and for the majority of the Sarbecoviruses. In line with these observations, a major fraction of the serum samples, including the selected three, show broad neutralizing activity against recent Omicron subvariants including XBB.1.5. This is in contrast with the results obtained with the sera from individuals receiving multiple doses of original and updated mRNA vaccines, where impaired neutralization of XBB and later variant of concerns was observed. Our study demonstrates that two doses of the ChAdOx vaccine in a highly exposed population was sufficient to drive

substantial neutralization breadth against emerging and upcoming variants of concern, thus paves the path towards the development of future vaccine candidates.

Importance

Worldwide implementation of COVID19 vaccine and parallel emergence of newer SARS-CoV-2 variants has shaped the humoral immune response in a population specific manner. While characterization of this immune response is important for monitoring the disease progression at population level, it is also imperative for the development of effective countermeasures in the form of novel vaccines and therapeutics. India has implemented the world's second largest COVID19 vaccination drive and also encountered large number of post vaccination "breakthrough" infections. From a cohort of breakthrough infection patients, we identified individuals whose sera showed broadly cross-reactive immunity against different SARS-CoV-2 variants. Interestingly, these sera primarily target a novel cryptic epitope which was not identified in previous population level studies conducted in western countries. This rare cryptic epitope remains conserved across all SARS-CoV-2 variants including the recently emerged ones and also for the SARS-like coronaviruses that may cause future outbreaks, thus representing a potential target for future vaccines.

Key Words: SARS-CoV-2, spike protein RBD, epitope mapping, breakthrough infection, convalescent serum, yeast display library, neutralizing antibodies, class-5/ RBD8 epitopes, immune escape, Omicron subvariant-XBB.1.5.

Introduction

Severe Acute Respiratory Syndrome Coronavirus 2 (SARS-CoV-2) has been circulating in the human population for over four years and rapidly evolving, causing the emergence of more than 50 different variants to date (1). Multiple waves of infections were caused by the new variants despite of massive vaccination programs, and their emergence was largely driven by the host immunity generated through natural infections and vaccination (2). Detailed molecular-level understanding of the humoral immunity conferred by different vaccination regimens coupled with ongoing viral exposures is important for the development of effective countermeasures against the current and future variants of SARS-CoV-2 and other Sarbecoviruses that may emerge in future.

More than 5.55 billion people, 72.3% of the world population, have received a single dose of COVID-19 vaccine (3), though in Africa, this number is less than 40% (4). India ranks second highest after China in the number of COVID-19 vaccine doses administered (2.2 billion doses) (5). The vaccination drive started in India on 16th January 2021, at the end of the first wave of infections caused mainly by the circulating B.1.1.7 (Alpha) and B.1.135 (Beta) variants. While the vaccination program was ongoing, the highly infectious B.1.617.2 (Delta) variant emerged and caused the second wave of the pandemic (March to October 2021), which resulted in the highest number of daily infections with high disease severity and mortality rate (6, 7). By January 2022, more than 77% of the Indian population were immunized; the new highly transmissible and heavily mutated B.1.1.529 (Omicron) variant emerged and led to the third wave of infection but was associated with milder symptoms and lower fatality rates (8). A significant fraction of the vaccinated population in India got infected during the second and third waves of the pandemic, leading to the large number of “breakthrough infections” (9). These breakthrough infections shaped the transmission dynamics and contributed to the overall evolution of the virus (10). After 2021, there was little vaccine uptake in the country and the percentage of the population that received a third (booster) dose was only about 10%.

The SARS-CoV-2 spike protein (S) is the main surface glycoprotein that mediates the interaction with the host angiotensin-converting enzyme 2 (ACE2) receptor and subsequent

95 fusion of the viral envelope with the host cell membrane that marks the initiation of the
96 infectious cycle (11, 12). The S protein is the primary target for neutralizing antibodies elicited
97 through natural infection as well as vaccination (13–15). The spike constitutes a trimer where
98 individual protomers are comprised of two subunits, S1 and S2 (16). S1 harbours the N-
99 terminal domain (NTD), the Receptor Binding Domain (RBD), and the S2 houses the fusion
100 peptide, the heptad repeats 1 and 2 (HR1, HR2), the transmembrane domain (TM) and the C-
101 terminal domain (CD). The majority of human neutralizing antibodies, isolated from
102 convalescent or vaccinated sera, target conformational epitopes in the RBD Receptor Binding
103 Motif (RBM) or in the conserved core of RBD (17–19) . In the context of the spike trimer, the
104 individual RBDs can be either in the up or down conformation, with only the former able to
105 bind the ACE2 receptor.

106 The epitopes targeted by neutralizing antibodies can be classified into four major
107 classes (Class 1-4) (20). Class 1 and class 2 epitopes overlap with the ACE2 binding site, and
108 antibodies targeting these sites competitively inhibit receptor binding. While class 1 epitopes
109 are accessible when RBD is present in the up conformation, class 2 epitopes are accessible
110 in both up and down conformations (21). For certain class 2 epitope targeting antibodies
111 (C144), the long complementary determining region (CDR) of the heavy chain acts as a bridge
112 between adjacent RBDs from neighbouring protomers in the down conformation, thus locking
113 the S trimer into the prefusion closed conformation; an unusual mode of neutralization (21). In
114 general, the antibodies targeting class 1 and class 2 epitopes have strong neutralizing activity.
115 However, different SARS-CoV-2 variants escape neutralization by these antibodies by
116 acquiring mutations in the RBM region that is part of the class 1 and 2 epitopes, compromising
117 their efficacy. Both class 3 and class 4 antibodies bind to the RBD core region away from the
118 ACE2 binding site. N343 glycan and the surrounding residues are accommodated in class 3
119 epitopes (22). S309 antibody, a class 3 antibody isolated from a SARS-CoV infected individual,
120 exhibited broad cross-reactivity against SARS-CoV and SARS-CoV-2, although many SARS-
121 CoV-2 VOCs acquired mutations in class 3 epitopes to escape neutralization by these
122 antibodies (21). The cryptic epitope around the RBD base (first described for CR3022

123 antibody) constitutes the highly conserved class 4 epitope and is accessible only in the RBD
124 up conformation (23–26). Despite their rare prevalence in convalescent sera, antibodies
125 targeting class 4 epitopes are suggested to protect against emerging VOCs and other
126 sarbecoviruses. Additionally, a highly conserved class 5 epitope has been recently identified
127 and characterized as a target for broadly neutralizing antibodies (27, 28).
128
129 Mapping monoclonal antibody epitopes can inform about viral evolution and aid in the
130 development of epitope-based vaccines and therapeutics. However, mapping conformational
131 epitopes targeted by polyclonal sera remains challenging. Mapping these epitopes can
132 elucidate how escape mutations in the viral antigen impact the neutralization potency of the
133 human polyclonal sera harbouring a heterogeneous mixture of antibodies. In the present
134 study, we have conducted a comprehensive analysis of human sera collected from individuals
135 vaccinated with two doses of the ChAdOx1 nCoV-19 viral vectored vaccine and subsequently
136 had undergone breakthrough infections. Neutralization efficacies of 164 sera samples were
137 screened against SARS-CoV-2 pseudoviruses representing the parental strain WA.1 or VOCs
138 B.1.617.1, B.1.617.2 and B.1.1.529. Nine individuals whose serum samples exhibited broader
139 neutralization were subjected to longitudinal sampling and three of them were selected for
140 epitope mapping due to their high neutralization breadth and potency. Utilizing charge
141 scanning mutagenesis (29, 30), a library of individual charged substitutions at all the solvent-
142 exposed positions of the wild-type RBD was generated and displayed on the yeast surfaces
143 to map the epitopes targeted by the polyclonal sera. A high fraction of antibodies targeting
144 either class 1 epitopes or the rare cryptic class 5 epitope, also denoted as RBD8 (31), were
145 observed in all three sera tested. The class 5/ RBD8 epitope residues identified in this study
146 are highly conserved across all SARS-CoV-2 variants, consistent with the observed
147 neutralizing potency of the selected serum samples against heavily mutated Omicron BA.1,
148 BA.5, and the recent XBB.1.5 variant. Our findings illustrate how a combination of vaccination
149 and breakthrough infections in a highly exposed population can elicit diverse antibody classes
150 that confer potent neutralizing activity with broad cross-reactivity. This in turn provides insights

151 into why deaths and hospitalizations have remained low post-2021 in virtually all low and
152 middle-income countries (LMICs) even in the absence of variant updated vaccine boosters.
153
154 **Results**
155
156 **Study cohort**
157 In contrast to vaccination alone, hybrid immunity resulting from SARS-CoV-2
158 breakthrough infections has been shown to boost neutralizing antibody titers while increasing
159 their breadth at the same time (32, 33). We selected individuals who received two doses of
160 the ChAdOx1 nCoV-19 viral vector vaccine between April and November 2021 and then were
161 infected between November 2021 and January 2022, which marks the transition between the
162 second and third waves of the pandemic in India, caused by the B.1.617.2 (Delta) and
163 B.1.1.529 (Omicron) variants, respectively (34) (Fig 1A, B). We hypothesized that such
164 individuals would have developed broadly cross-reactive neutralizing antibodies that are
165 effective against different variants of concern (32, 33). Blood samples, along with
166 questionnaires about gender, age and symptoms, were collected from 164 selected individuals
167 who were voluntarily recruited by a separate consent for this study. All participants were
168 confirmed positive by RT-PCR for SARS-CoV-2 infection during the abovementioned time
169 frame, which is within 2-4 months post-second dose of vaccination. The serum samples were
170 collected from the individuals within 4-6 weeks of their breakthrough infection (Fig 1A, B). The
171 study cohort consisted of 90 males and 74 females; the median age was 36 and 34 years,
172 respectively (Fig 1C). Most volunteers showed mild symptoms like fever, head and body ache,
173 cough, chest congestion and loss of smell with no cases of hospitalizations. Only 5.84% (10
174 individuals) of the individuals showed severe to critical illness with declining oxygen saturation
175 and breathlessness along with abovementioned symptoms.
176
177 **Neutralization profile of the polyclonal serum samples against SARS-CoV-2 variants.**

We employed a high throughput neutralization assay based on reporter lentiviruses pseudotyped with spike proteins from SARS-CoV-2 parental WA.1, B.1.617.1 (Kappa), B.1.617.2 (Delta) and B.1.1.529 (Omicron) strains (35). For human convalescent sera, such pseudoviruses show neutralization titers comparable to the live SARS-CoV-2, thus can serve as an effective proxy for the live virus neutralization assay (36). Pseudoviruses were incubated with dilutions of serum samples ranging from 10^{-2} to 10^{-4} before infecting HEK-293T cells overexpressing ACE2. The reporter signal was measured as a proxy of the infectivity, which was the highest for the mock-treated cells and the lowest for a polyclonal antibody preparation that binds the spike protein and has high neutralization activity (Novus Biologicals, NB100-56578). The neutralization efficacies of 164 serum samples (all three dilutions) against WA.1 and different VOCs was represented as a heatmap with colours ranging from red (high neutralization) to green (low neutralization) (Fig 2A). Overall, the serum samples from this study exhibited maximum neutralizing activity towards the Delta variant followed by the Kappa variant with a geometric mean (GM) of 93% and 90%, respectively (Fig 2B). Reduced neutralizing activity was observed against the parental WA.1 strain (GM-73%), which was further lowered against the Omicron variant (GM-46%) (Fig 2B). These results suggest that the majority of the individuals in the study cohort had breakthrough infections caused by the Delta variant. Most of the serum samples neutralized Delta and Kappa variants to similar extents, which was better than WA.1 (Fig 2A, B), likely due to the high similarity between the spikes of both variants (37). Interestingly, certain sera (BCRTH 29, 30, 33, 35, 45, 46) showed potent neutralization against WA.1 but failed to neutralize other tested VOCs, especially at higher dilutions (Fig 2A). This suggests that for certain individuals, vaccination and subsequent infections have induced a strong immune response towards the parental strain but failed to generate antibodies that are broadly cross reactive against the VOCs, as also reported previously (38). A few serum samples showed high neutralization activity against the Omicron variant (Fig 2A, B). Limited neutralization activity against the Omicron variant results from the high number of mutations conferring extensive immune escape from vaccine and infection sera (39).

The breadth and cross-reactivity of the selected polyclonal serum.

In the initial screening, 29 out of the 164 breakthrough infection sera (17%) showed broadly cross-reactive neutralizing activity against WA.1, Kappa, Delta and Omicron variants at 10^{-2} dilution (Fig 2C & Fig 2A, red diamonds); hence, were considered as broadly neutralizing serum samples. We tracked these 29 individuals, and selected 9 volunteers who had not been infected and had not received any vaccine booster post the first round of blood collection. Subsequently, second set of serum samples (designated “late”) were collected from the 9 selected individuals with proper consent, 4-6 weeks post the first set (designated “early”) (Fig 1A, B), and both early and late sets of serum samples were subjected to further analysis.

Neutralization efficacies of the selected serum samples were determined against WA.1, Delta and the Omicron variants using the pseudovirus neutralization assay (Fig S1, A, B) and neutralization titers were represented in the form of IC_{50} (Fig 3A, B). Amongst the nine serum samples collected at the early time point, four showed the highest IC_{50} values for Delta, three for the parental WA.1 strain and two for the Omicron; a trend that matched with the overall neutralizing activity of the larger cohort of 164 samples (Delta> WA.1> Omicron; Fig 2B). Interestingly, this was not the case for the serum samples collected from the same volunteers at the later time point (Fig 3A, B). A moderate to sharp decline in neutralizing activity (2-18 fold change in IC_{50}) was observed for most serum samples between early and late time points (Fig 3 C, D). Interestingly, a few sera had an increase or maintained similar variant-specific neutralization titers at both time points. Compared to the early time point neutralization profile, BCRTH01 and INK41 showed a significant decline in neutralization titer against WA.1 but a slight increase in neutralization titer against the Omicron variant, at the late time point (Fig 3 C, D). This may reflect the higher durability of the variant specific (Omicron or Delta) antibodies generated by the breakthrough infections with respect to the parental strain (WA.1) specific antibodies elicited through vaccination. Interestingly, BCRTH01, INK09, INK36 and

INK41 sera maintained high neutralization titers against all the pseudoviruses tested and at both time points, with INK36 being the most potent neutralizing sera (Fig 3C, 4C and Fig 5B).

As the majority of the neutralizing antibodies target the receptor binding domain (RBD) of the spike protein (17–19), we sought to test the binding activity of the four serum samples (BCRTH01, INK09, INK36 and INK41) to the spike RBD. Enzyme-linked immunosorbent assay (ELISA) was performed with recombinant purified spike RBD derived from the WA.1, Omicron BA.1 and BA.5, which are used as coating antigens. As expected, all four serum samples bound well to the RBD, with the BCRTH-01 sera showing highest binding affinity for all three RBD variants. This suggests high abundance of RBD-targeted antibodies in the selected convalescent serum (Fig 4 A). In general, the serum samples showed highest IgG titres against WA.1 and marginally lower titres against BA.1 and BA.5 (3– 4.2 fold reduction) (Fig 4B, C). BA.5 RBD exhibited higher sensitivity than BA.1, but lower sensitivity than WA.1 for binding to all four serum samples tested. As all of the four serum samples showed comparable neutralization titers against RBD, we selected three of them, namely BCRTH01, INK09 and INK36, for epitope mapping study.

Comprehensive mapping of RBD epitopes targeted by the selected human serum.

We employed a charged scanning mutagenesis library of SARS-CoV-2 RBD displayed at the yeast surface as a novel approach to identify the epitopes targeted by the antibodies present in the polyclonal serum samples (Fig 5A). WA.1 RBD (332-532) was used as the template for library construction and all RBD residues with solvent accessibility >15% were individually mutated to negatively charged Aspartate, with the exception of negatively charged residues, which were mutated to the positively charged Arginine. The generated RBD library was displayed on the yeast surface and subjected to binding with a saturating concentration of the polyclonal serum sample as determined by sera titration on the yeast surface (Fig S2 A). Binding was detected using fluorescently labelled antibodies, and the yeast cell populations were sorted into different bins through Fluorescence Activated Cell Sorting (FACS) (FigS2, B-

D). Yeast populations within these bins were subjected to deep sequencing to identify the mutations responsible for abolishing binding to the serum. The deep sequencing reads were analyzed as described in the methods section. Briefly, the binding and expression signals of each mutant RBD were normalized with respect to the wildtype and the MFI ratio between the normalized Mean Fluorescence Intensities for expression (MFI-expression) and binding (MFI-binding) for each of the RBD variants was calculated.

Epitope mapping was performed with all three of the selected serum samples (BCRTH01, INK09 or INK36) and RBD residues whose mutation resulted in MFI_{Ratio} one standard deviation higher than the mean MFI_{Ratio} were considered epitopes (Fig 5B, Table 1). A high value of MFI_{Ratio} (darker shades of red) indicates that the charged substitution significantly perturbed the binding of the serum samples with minimum or no effect on expression. The MFI_{Ratio} of the identified epitope residues were mapped on the RBD structure (Fig 5C). Overall, the identified epitopes (highlighted in lighter to dark shades of red) for all three serum samples were clustered in two major groups; (i) epitopes that overlap with the ACE2 binding motif (RBM- designated by black line on the RBD structure, Fig 5C) and (ii) epitopes that are away from the RBM. Interestingly, for BCRTH01 serum, an enrichment in non-RBM over RBM epitope residues was observed. However, this was not the case for INK36 or INK09, where epitope residues across different RBD regions were enriched to similar levels (Fig 5C).

To this end, we aimed to validate the results of the yeast-display screening and deep sequencing, by individually mutating the epitope and non-epitope residues in RBD and evaluating their impact upon serum binding. Considering that validating all of the library residues would be difficult, we selected three epitope and three non-epitope residues that are identified in the context of all three serum samples (BCRTH-01, INK-09 and INK-36) and reintroduced these mutations into the RBD individually. Subsequently, extent of binding of these mutant RBDs by all three serum samples were evaluated by yeast surface display

followed by flow cytometry (Fig S3 A-C). We selected the non-RBM epitope residues (T430, T437 and R466) as they showed high values of MFI_{Ratio} compared to the wildtype. As shown, charged substitution at the putative epitope residues significantly impacted the binding to the serum samples while charged substitution at putative non-epitope residues had no effect upon the binding (Fig 5 D). The impact of mutating the epitope residues was most prominent for BCRTH-01 and higher than INK-09 and INK-36, possibly because of the highest abundance of the RBD specific antibodies in BCRTH-01 serum. This data validates the epitope residues identified through the current study and establishes the robustness of the charged scanning mutagenesis approach for the identification of epitope residues targeted by polyclonal human serum.

Antibodies in the selected sera target a cryptic epitope that is broadly conserved across different SARS-CoV-2 variants.

Previous epitope mapping studies on convalescent polyclonal serum samples showed enrichment of antibodies targeting the class-1, -2 and -3 epitopes and to a lesser extent the class-4 epitope (39–43). Hence, we analysed the different epitopes identified in the present study and compared them to the epitopes reported in the literature. The majority of the neutralizing epitope residues in the RBD are categorized into four major classes, class 1-4 (Fig 6 A and Table 2). Out of the 26 epitopes residues identified, eight were classified as Class 1, two as Class 2, two as Class 3 and five as Class 4. Surprisingly, 11 out of the 26 (42%) epitope residues do not belong to any of these major classes (except for K356 which is shared with class 3 and T470 which is shared with class 2), but instead belong to a rare epitope (44, 45), situated away from the receptor binding motif of RBD (Fig 6A). These residues are part of a recently identified cryptic epitope designated as a class 5 or RBD8 class epitope. (31).

. The class 5 or RBD8 epitope spans diagonally across the base of the RBD (Fig 6A) and is situated on the opposite surface of the ACE2 binding motif, thereby remaining buried and inaccessible in the prefusion closed conformation of the spike trimer (Fig 6B). Hence,

binding of class 5 antibodies, such as BIOLS56, IMCAS74, WRAIR-2063/ S2H97/ WRAIR-2057/ WRAIR-2134, to this rare epitope requires extensive opening of the pre-fusion structure, thereby inducing rapid and premature transition to the post-fusion conformation and S1 shedding (27, 31, 46, 47). These antibodies cross-reacted with all SARS-CoV-2 VOCs, including Delta, Omicron BA.4/BA.5, BQ.1.1, and the recent highly immune escaping variant XBB1(31, 46). Supporting this notion, class 5 epitope residues identified in our analysis were highly conserved across all the different SARS-CoV-2 VOCs (Fig 6C) and also across different Sarbecoviruses (Fig S4). All these data together highlights the class 5 antibodies as potential broadly cross reactive universal vaccine candidate against SARS-like betacoronaviruses. Interestingly, the BCRTH01 serum had the highest number (total 10) of class 5 identified epitope residues compared to the INK09 and INK36 (7 and 8 residues, respectively) (Fig 6A, Table 2), which explains its breadth and high cross-reactivity against the different SARS-CoV-2 variants tested. In contrast, INK36 has the highest number of class 1 and class 2 epitopes (8 and 2, respectively) that are targeted by ACE2 competing antibodies, consistent with its highest neutralization activity amongst the three selected serum samples.

To evaluate the effect of charged substitutions on neutralizing activity of the polyclonal sera, we selected four of the identified RBD-epitope residues and individually mutated them to charged substitutions in the WA.1 backbone to generate mutant pseudoviruses. Two mutations, R403D and G416D, are situated within the RBM and are expected to perturb class 1 or class 1/ 4 epitope-specific antibodies, respectively while the other two mutations, T430D and R466D, are situated away from the RBM. T430D is expected to interfere with the binding of class 4 and class 5/ RBD8 epitope-specific antibodies, while R466D is expected to exclusively disturb the latter (Fig 6C, Table 2).

We tested the sensitivity of WT and mutant pseudoviruses to neutralization by BCRTH01, INK09 and INK36 serum (Fig 7A). As expected, all of the mutations reduced the neutralization activity of all three polyclonal serum in comparison to the WT pseudovirus. BCRTH01 showed highest sensitivity towards R466D and R403D mutations with drastic 132-fold and 48.9-fold

reduction in the neutralization titer (IC_{50}), respectively (Fig 7 B). In contrast, T430D and G416D mutations showed moderate and comparable effects with 3.55- and 4.12-fold reduction in IC_{50} values, respectively. On the other hand, INK36 showed high 35.5-fold and 27.8-fold reduction towards R403D and G416D mutations, moderate 11.5-fold reduction towards R466D mutation and negligible 1.3-fold reduction for T430D mutation respectively. INK09 showed same trend as INK36, but with less prominent reductions towards the abovementioned mutations. It is to be noted that T430 residue has been identified as epitope for BCRTH01, but not for the INK09 or INK36 serum samples and hence its mutations showed negligible reduction towards the neutralization titers of the these two sera. Together, our data suggests that the BCRTH01 sera harbours the highest fraction of class 5/ RBD8 and class 1 antibodies while the INK36 and INK09 possesses higher fraction of class 1 and class 4 antibodies and lower fraction of the class 5/ RBD8 antibodies. This combination of ACE2 competing (class 1) and non-competing (class 5/ RBD8 and class 4) antibodies imparts high neutralization efficacy and broad cross reactivity to all of these serum samples, which render it effective against different variants of SARS-CoV-2, including the currently circulating ones.

Pre-XBB serum neutralizes the recent Omicron subvariant XBB.1.5.

The heavily mutated Omicron subvariant, XBB and XBB.1, emerged in late 2022 and soon, XBB and its descendants accounted for the majority of infections in the whole world (48, 49). The variant XBB.1.5 harbours a rare mutation, F486P, which demonstrates superior transmissibility and immune escape towards vaccines and monoclonal antibodies, accounting for its rapid spread in more than 100 counties (50–55). Interestingly, the epitopes identified in this study remain completely conserved for XBB.1.5 (Fig 6C), suggesting that the selected serum samples should neutralize this more recent subvariant of SARS-CoV-2. Thus, we generated pseudoviruses harbouring either WA.1, Omicron BA.1 or Omicron XBB.1.5 spike proteins at their surface and performed neutralization assays with the BCRTH01, INK36 and INK09 serum samples which were collected in early 2022, well before the emergence of XBB.

Interestingly, all three serum samples showed neutralizing activities against Omicron BA.1 and XBB.1.5 comparable to the parental WA.1 strain (Fig 8A).

It is possible that the XBB.1.5 neutralization activity showed by the three selected serum samples may be an outcome of random stochasticity and do not represent a general trend of the larger study cohort. To investigate this, we evaluated the neutralizing activity of the all 29 serum samples, which showed broader cross-reactivity against all of the tested SARS-Cov-2 variants in the initial screen (Fig 2C). WA.1 or the XBB.1.5 pseudoviruses were neutralised with different concentration of the serum samples (Fig S5) and the respective neutralization titers are plotted in Fig 8B. As evident, all of the serum samples showed comparable neutralizing activity towards WA.1 and XBB.1.5 with a maximum of 7 fold reduction for the later. This data indicates that a significant fraction (17%) of the participating volunteers, who had breakthrough infections following vaccination during the Delta/ Omicron wave (December 2021) of the pandemic, generated humoral immunity that remained effective even against recently emerged subvariants (February-March 2023). This, in turn, establishes the potential importance of the identified epitopes as a target for developing vaccine candidates against future SARS-CoV-2 variants.

Discussion.

Hybrid immunity generated by breakthrough infections have been reported to induce enduring humoral immunity and generate broadly neutralizing antibodies (33, 56, 57) against SARS-CoV-2 variants through several different mechanisms (58). First, vaccination and infection select different B cell clones leading to the generation of broadly cross-reactive neutralizing antibodies (59, 60) . Second, the antibodies generated through primary antigen response directly modulate the secondary response against SARS-CoV-2 by blocking or enhancing the naïve B cell recruitment (61). Third, timely spaced repeated antigen contacts through vaccination and subsequent infection promote more extensive germinal centre reactions resulting in high affinity cross-reactive neutralizing antibodies (62, 63). These

398 together explains why breakthrough infections with specific omicron variants activates specific
399 memory B cells that recognizes conserved cross-variant epitopes rather than promoting naïve
400 B cell recruitment (64, 65). In this study we examined the hybrid immunity and characterized
401 the epitopes targeted by the antibodies generated in a small cohort of breakthrough infection
402 patients from India.

403 Human high-resolution epitope mapping studies following vaccination and/or infection have
404 been largely focused on sera from US or European populations that were primarily immunized
405 with mRNA vaccines (19, 43, 66, 67) while a few studies focused on sera from individuals
406 vaccinated with CoronaVac whole virus inactivated vaccine, with or without breakthrough
407 infection (54, 68, 69). Little is known about the humoral response in LMICs and China, which
408 are home to ~85% of the world's population. In the present study, we describe epitope
409 mapping of sera from an Indian population where participating volunteers received two doses
410 of viral vector vaccine and had a "breakthrough infection" within 4-6 weeks post-second dose.
411 The timing of the study was deliberately chosen at the intersection of the second and third
412 waves of the pandemic instigated by the B.1.617.2 (Delta) and B1.1.529 (Omicron) variants,
413 which, in theory, were expected to enhance the breadth and potency of antibodies generated
414 through vaccination (parental strain WA.1) and subsequent infections by different VOCs (33).
415 Around 18% of the serum samples exhibited > 65% neutralizing activity against the parental
416 strain and different VOCs including Kappa, Delta, and Omicron (Fig 2C). Furthermore, via
417 longitudinal sampling, three serum samples were identified that not only maintained their
418 broad neutralizing activity up to 12 weeks post-infection but also demonstrated effectiveness
419 against the recent circulating Omicron subvariant XBB.1.5. Although prior exposure to
420 Omicron spike, including BA.1 bivalent vaccination has been reported to generate XBB.1.5
421 specific antibodies (70), the neutralizing activity remained low compared to the parental WA.1
422 or D614G strains (52, 70–72). Several studies have demonstrated a substantial escape of
423 XBB variants from neutralization by convalescent and vaccinated sera, with more than 20-fold
424 reduction in neutralization titres compared to WA.1 (41, 54, 71, 73). Strikingly, 29 out of 164
425 (18%) broadly cross reactive serum samples (from Fig 2C) showed comparable WA.1 and

426 XBB.1.5 neutralizing titers (≥ 7 fold reduction for XBB.1.5) (Fig 8B), hence representing proof
427 towards the role of hybrid immunity in generating highly potent, durable, and broadly cross-
428 reactive neutralizing antibodies.

429 We employed an aspartate scanning mutagenesis and yeast surface display coupled
430 with flow cytometry and deep sequencing to map epitope residues which, upon charged
431 substitution, severely impacted the binding of the serum antibodies without affecting the
432 expression. Charge scanning mutagenesis has been previously proven to be effective in
433 identifying residues buried at protein-protein interaction interface (74, 75). While Deep
434 Mutational Scanning has been previously employed to identify serum escape mutations on
435 SARS-CoV-2 RBD (19, 76), the relatively smaller size of the aspartate scanning library,
436 together with the unique barcoding strategy of the individual mutant ORFs employed by us
437 simplify library construction and downstream analysis. Using this method, we identified a total
438 of 26 surface-exposed amino acid residues as potential epitopes targeted by the sera. The
439 majority of these residues have been previously identified as part of epitopes for different
440 classes of RBD neutralizing monoclonal antibodies (77), thus supporting the robustness of the
441 novel screening approach in identifying epitopes targeted by polyclonal sera.

442 The epitopes identified using the proposed analysis can be broadly categorized into
443 two main groups: RBM epitopes overlapping with the ACE2 binding motif and non-RBM
444 epitopes. The RBM epitopes consist primarily of class 1 and class 2 epitopes which are
445 targeted by antibodies that competitively hinder receptor engagement and virus attachment to
446 host cells. While antibodies targeting these epitopes are responsible for the high neutralizing
447 activity of polyclonal serum used in this study (17, 21, 78–80), higher frequencies of escape
448 mutations in these regions limits their breath and cross-reactivity in the emerging VOCs (25,
449 26, 47, 81). For example, the R403K mutation, in the class 1 epitope, has been classified as
450 “vaccine escape mutation”, leading to higher infectivity and lower neutralizing activity of
451 vaccine-elicited antibodies against the recent JN.1 subvariant of Omicron (82). Interestingly,
452 the R403D mutation resulted in 48.9 fold reduction in neutralizing activity of the BCRTH01

serum as evidenced in our study. Another identified class 2 epitope residue substitution L452R, was associated with a massive expansion and immune escape of the Delta variant from vaccine-elicited class1 and class 2 antibodies (43) during the second year of the pandemic (83). Similarly, the F456L mutation (class 1 epitope) is associated with heightened ACE2 binding, infectivity, and immune evasion from the XBB.1.5 neutralizing antibodies (84) leading to the global spread of EG.5 (Eris) subvariant (85) in the recent past. The K356T mutation in JN.1, in the class 3 epitope, drives resistance towards Sotrovimab, a class 3 antibody (S309) based antiviral drug (86). In contrast to classes 1-3, the class 4 epitopes targeted by the selected sera described above show high conservation (Fig 6C). These class 4 epitopes are situated in the RBD core region, away from the RBM except for the G416, which resides within RBM. Class 4 antibodies targeting G416 (COVA1-16, C118 and C022) and surrounding residues sterically hinder ACE2 binding (25, 26) thereby resulted in high neutralizing activity.

A major fraction (11/26) of the epitope residues identified in the present study belong to a newly identified epitope (44, 45, 87), rarely seen in the repertoire of antibodies from convalescent sera (40–43). Recently, this epitope has been categorized as class 5 or the RBD8 class of epitopes (27, 31). These antibodies are reported to get enriched by breakthrough infections caused by Omicron subvariants (54). The amino acid residues constituting these epitopes are clustered together at the opposite surface from the ACE2 binding motif of RBD and remain inaccessible in the closed trimeric form of the spike (S) (Fig 6B). Such epitopes can only be accessible through breathing of the prefusion structure of the trimeric S protein (Fig 6B) whereby antibody binding ultimately leads to shedding of the S1 subunit (31). Additionally, it has been proposed that the binding of class 5 antibodies leads to premature, receptor-independent conversion of S from pre- to post-fusion conformation, ultimately blocking viral entry and syncytium formation (88). Interestingly, class 5 epitope residues remain completely conserved across all SARS-CoV-2 variants and for a number of different Sarbecoviruses, indicating the cross-reactivity and increased breadth of class 5 antibodies against these viruses. Consistent with this, the selected serum samples, enriched

for RBD8 epitope antibodies, effectively neutralized WA.1, Delta, Kappa, Omicron BA.1 and XBB.1.5.

Lately, antibodies targeting non-RBM epitopes in the spike protein have emerged as prime candidates for developing broad-spectrum vaccines or therapeutics against SARS-CoV-2 variants (28, 89, 90). Some of these antibodies showed cross reactivity against different Sarbecoviruses, thus further extending the prophylactic/therapeutic potential of such antibodies against future emerging SARS-like coronaviruses. However, non-RBM antibodies are limited by their weak neutralization activity. Rao et al., have shown that the RBD8 antibody (BIOLS56) can rescue the immune escape caused by an RBM targeting antibody (IMCAS-L4.65), together ensuring strong neutralizing activity and broad neutralizing efficacy against different Omicron variants (31). In this study, we show that an immune response elicited by hybrid immunity and containing a combination of class-1 (RBM targeting) and class 5/ RBD8 antibodies can achieve neutralization potencies against different SARS-CoV-2 variants including WA.1, Kappa, Delta and multiple Omicron subvariants including the more distant XBB.1.5. Characterizing such combination of different classes of antibodies is important for optimizing novel vaccine recipes against existing and yet to be emerging sarbecovirus. Interestingly, mutation of a single class5/ RBD8 epitope residue (R466D) resulted in 132 fold reduction in the neutralization titer, which is even higher than that observed in the case of mutations of class 1 (R403D) epitope (48.9 fold), suggesting high abundance and comparable neutralization efficacy of these two different classes of antibodies (class 5/ RBD8 and class 1) in the one of the selected serum samples (BCRTH01) used for epitope mapping analysis. This contrasts with the previously conducted epitope mapping studies from the convalescent polyclonal serum samples, which led to the identification of class 1-4 epitope targeting antibodies (40–43).

In conclusion, antibodies targeting different classes of epitopes may synergistically contribute to achieving high neutralizing activity (Class 1+2 epitopes) and broader cross-reactivity (Class 4 and RBD8) against all variants of SARS-CoV-2. Notably, RBD8 constitutes

a significant portion of the epitopes identified in all three serum samples, which differs from the typical composition of the convalescent serum samples analysed previously (40–43). In India, after the Delta wave in mid-2021, there was little masking or isolation, and likely continued extensive viral exposure. This, coupled with the relatively young population (median age 28.4 years) may have contributed to the generation of broadly cross reactive antibodies targeting novel cryptic epitope presented here. These findings need to be confirmed in larger epitope mapping studies where the humoral immune response, abundance of specific classes of antibodies should be correlated with the clinical manifestation of the disease. Greater understanding of this adaptive strategy implemented by the host would pave the way towards the development of universal vaccines and therapeutics against newly emerging SARS-CoV-2 variants and future sarbecovirus outbreaks.

Materials and methods

Cell line

Human embryonic kidney (HEK) 293T cells (ATCC #CRL-3216) were maintained in Dulbecco's modified Eagle's medium (DMEM) supplemented with 10% fetal bovine serum (FBS) along with antibiotics like penicillin, streptomycin and anti mycotic agent (Gibco) at 37°C and 5% CO_2.

Plasmids:

Plasmid pHAGE2-EF1aInt- ACE2-WT, expressing human ACE2 gene (BEI#NR-52514) was used for overexpressing ACE2 in HEK 293T cells. Plasmid HDM-IDTSpike-fixK (BEI#NR-52514) was used for expressing the codon-optimized spike protein from SARS-CoV-2, Wuhan-Hu-1 strain (Genbank NC_045512). Plasmids pcDNA3.3-SARS2-B.1.617.1, expressing spike protein of Kappa variant (addgene#172319), pcDNA3.3-SARS2-B.1.617.2 SARS-CoV-2, expressing spike protein of Delta variant (addgene#172320) (91) and SARS-

535 CoV-2 Omicron strain spike gene in Human codon_pcDNA3.1(+) expressing spike protein of
536 Omicron variant (B.1.1.529) (GenScript# MC_0101274) were utilized in the study (35). XBB1.5
537 spike expression plasmid construct was a kind gift from Dr. Rajesh P. Ringe, Institute of
538 Microbial Technology, Council of Scientific and Industrial Research (CSIR), India.
539
540 **Antibodies:**
541 NB100-56578 is a polyclonal antibody raised in rabbits against SARS CoV-2 spike
542 protein and was obtained from Novus Biologicals (USA). Serum from the pre-COVID era
543 (Single donor human serum off the clot, ISERS2M-2019-33108-07) was obtained from
544 Innovative Research, Inc.
545
546 **Bioinformatics and Structural Analysis:**
547 Genome sequences of 47 different SARS-CoV-2 viruses that infect humans and 11
548 different sarbecovirus spike RBD sequences were obtained from the GISAID database.
549 Multiple sequence alignment was performed in Bioedit software using ClustalW multiple
550 alignment function. Further representation of the spike proteins' aligned RBD amino acid
551 sequences was performed using JALVIEW or the Multlin sequence alignment tool. Structural
552 alignment was performed in Pymol using specific PDB files of post-fusion spike protein
553 structures of SARS-CoV-2 viruses (PDB id: 6M0J).
554
555 **Construction of SARS-CoV-2 S mutant plasmid constructs:**
556 Plasmid HDM-IDTSpike-fixK expressing a codon-optimized spike protein from SARS-
557 CoV-2 was subjected to site-directed mutagenesis to generate R403D, G416D, T430D and
558 R466D, respectively, using the QuikChange II Site-directed mutagenesis kit (Agilent) according
559 to the manufacturer's instructions. Mutations generated in the SARS-CoV-2 S protein were
560 further verified using Sangers sequencing.
561
562 **Generation of SARS-CoV-2 S pseudotyped lentiviruses:**

Generation of SARS-CoV-2 lentivirus particles pseudotyped with either full-length WT, different VoCs or mutation at SARS-CoV-2 spike protein (R403D, G416D, T430D and R466D) were generated by transfecting HEK293T cells with the respective set of plasmids by using the protocol as described previously by Crawford et al., 2020 (92). Briefly, a lentiviral backbone plasmid, pHAGE-CMV-Luc2-IRES-ZsGreen-W (BEI #NR-52516) bearing a CMV promoter to express luciferase, was co-transfected with a set of other lentiviral plasmids like pHDM-Hgpm2, expressing the HIV-1 gag and pol (BEI #NR-52517), pRC-CMV-rev1b, expressing the HIV-1 rev (BEI #NR-52519), pHDM-tat1b, expressing the HIV-1 tat (BEI # NR- 52518), and respective different WT or mutant spike protein-expressing plasmids. Post transfection, the SARS CoV-2 pseudoviruses were collected by passing the supernatant through a 0.45 um filter and used freshly.

Pseudovirus-based Serum Neutralization Assay:

Serum samples collected from the volunteers were inactivated at 65^0C for 30 minutes prior to use. Serially diluted serum samples were incubated with either WT or different VoC/ mutant pseudoviruses at 37^0C for 1h. Serum-neutralized viral inoculum was then used to infect hACE2-expressing HEK 293T cells at 37℃ for 1h in the CO_2 incubator in the presence of polybrene till 18h. Successful neutralization of the pseudovirus results in a several fold reduction in reporter virus activity, which were measured using a multimodal plate reader (GloMax® Explorer Multimode Microplate Reader, Promega). Polyclonal SARS CoV-2 (NB100-56578) antibody served as a positive control, whereas sera from the pre-COVID era were used as a negative control for the study.

Charged scanning library construction and yeast surface display:

Substitutions to Aspartate and Arginine are chosen for introduction in scanning mutagenesis as analysis of existing DMS data suggests that these are the most disruptive for binding. A charged scanning library of SARS CoV-2 spike RBD was generated using site-directed mutagenesis. Exposed positions with accessibility >15% (total 125 residues) were

591 individually mutated to Aspartate or Arginine (for negatively charged residues), and each
592 mutant was fused by PCR to a unique 6 nucleotide barcode of known sequence to simplify
593 analysis and eliminate the need for long read sequencing. Upon mutagenesis by overlap PCR,
594 all the PCR products from each individual mutated position were pooled and transformed into
595 yeast via two fragment recombination by electroporation.
596
597 **Human sera screening**
598 Three human sera were selected for screening based on their high neutralization titres.
599 The sera were first titrated on yeast surface displaying WT-RBD and a saturating concentration
600 was chosen from the titration curve to be used for epitope mapping. The binding of these sera
601 with the aspartate library was analysed by flow cytometry, sorted into multiple gates and then
602 subjected to deep sequencing. Briefly, the pooled library of yeast cells expressing each of the
603 charged mutants was inoculated in 5 ml of SDCAA medium and grown overnight at 30°C, 250
604 rpm. The next day, a secondary inoculation from the overnight culture of the library was grown
605 at 30°C until an OD600 of 3–4, followed by induction in SGCAA medium at 20°C for 16 hr. A
606 total of 1×10^7 cells of this library were washed twice with FACS buffer (1XPBS, pH 7.4 and
607 0.5% BSA) and then incubated at 4°C for 1 hr with a selected dilution of sera to probe for
608 binding and chicken anti-CMyc antibody (1:300 dilution) as a probe for the expression. The
609 cells were washed twice with FACS buffer and subsequently labelled with Alexa Fluor 633 goat
610 anti-human (1:1200 dilution) (catalogue no. A21091), plus Alexa Fluor 488 goat anti-chicken
611 (1:300 dilution), (catalogue no. A11039) for 20 min at room temperature in the dark. After
612 washing thrice with FACS buffer, cells were resuspended in 1 mL of FACS buffer, subjected to
613 flow cytometry, and sorted on an Aria-III cell sorter (BD Biosciences).
614
615 **Deep sequencing and analysis**
616 The sorted yeast cells from each gate were grown separately in liquid SDCAA medium
617 to saturation at 30°C for 24 hr, and the plasmids were extracted using EZ Yeast plasmid
618 miniprep kit (G Biosciences) according to the manufacturer's instructions and then subjected

619 to PCR. The PCR primers were designed to amplify the barcode region only (150 bp) and in a
620 way such that for both, the forward and reverse end reads, the first 3 bases are NNN followed
621 by 6 bases of unique sequence tag (MID) and the 21 bases of the primer sequence
622 complementary to the gene. Each forward MID sequence represents a particular serum, while
623 each reverse MID sequence represents a specific gate. The PCR for all the gates from three
624 sorted sera samples was carried out using Phusion polymerase for 15 cycles. Following
625 agarose gel electrophoresis and gel band purification, an equal amount (~100 ng) of PCR
626 product from each sample was pooled and then gel-band purified, followed by sequencing on
627 the NovaSeq platform. The fraction of each mutant (*Xi*) distributed across all the bins was
628 calculated as in (Equation 1) and then the reconstructed MFI for each mutant was calculated
629 by the summation of the product obtained from multiplying the fraction of a particular mutant
630 in a particular gate (*Xi*) with the MFI of that gate that was obtained from the FACS experiment
631 (*Fi*), (Equation 2).

632 Fraction of mutant in each gate $X_i = \frac{N_i}{\sum_1^n N_i}$ (Equation 1)

633 N*i*: Number of reads of a specific mutant in bin *i*.

634 Reconstructed MFI= $\sum_1^n X_i * N_i$ (Equation 2).

635 The ratio of MFI expression/MFI binding for all positions was represented by a heat map using
636 GraphPad Prism software. The mutants with Ratio (Normalized MFI of expression: Normalized
637 MFI of binding), one standard deviation higher than the mean MFI were considered as epitope
638 residues.

639 **Statistical analysis:**

640 All experiments were performed in triplicates, and each data was repeated at least
641 three times except for the epitope mapping experiments, which were performed in
642 duplicates. Graphs are plotted using Graphpad Prism 10.1.2 and represented as mean
643 standard deviations (n = 3). Results were compared by performing a two-tailed Student's t-test.
644 Significance is defined as $P < 0.05$, and statistical significance is indicated with an asterisk (*).
645 *$P < 0.001$ were considered statistically significant.

Acknowledgements:

Authors sincerely acknowledge the contribution of the volunteers participating in this study. The authors also acknowledge staffs of the medical institutions who were involved in this study for support in blood sample collection and handling.

Funding

This work is primarily supported by a grant from Indian Council for Medical Research (VIR/COVID-19/19/2021/ECD-I) awarded to A.M. and another grant from Bill and Melinda Gates Foundation (INV-042471) awarded to RV. AM also acknowledges the Science and Engineering Research Board (SERB-DST (CRG/2022/003628) for providing additional financial support. R.V. is a JC Bose Fellow of DST. RV also acknowledges infrastructural support was from DST FIST, MHRD, and the DBT IISc Partnership Program. I.D.J. acknowledges the Science and Engineering Research Board (SERB) for the National Post Doctoral Fellowship (PDF/2023/000284). K.K. acknowledges the support of an MHRD-IISc doctoral fellowship. The funders had no role in study design, data collection and interpretation, or the decision to submit the work for publication.

Authors' Contribution:

Conceptualization—A.M., and R.V. Designing experiments—A.M., R.V., I.D.J. and K.K. Performing experiments—I.D.J., K.K., and S.R. Manuscript writing—A.M., R.V., I.D.J. and K.K. Fund acquisition—A.M., R.V., B.M., and S.C. Manuscript editing— A.M., R.V., I.D.J. and K.K., B.M., and A.C. Deep Sequencing reads processing—M.B. Medical supervisors in cohort identification and blood collection—S.J., A.C., and I.B.

Declaration of interests: The authors declare no competing financial interests or dispute in the relationships that could have appeared to influence the work reported in this article.

References:

1. Ecdc.europa. https://www.ecdc.europa.eu/en/covid-19/variants-concern.
2. Zabidi NZ, Liew HL, Farouk IA, Puniyamurti A, Yip AJ, Wijesinghe VN, Low ZY, Tang JW, Chow VTK, Lal SK. 2023. Evolution of SARS-CoV-2 Variants: Implications on Immune Escape, Vaccination, Therapeutic and Diagnostic Strategies. Viruses https://doi.org/10.3390/v15040944.
3. Our world in data. https://ourworldindata.org/covid-vaccinations. covid 19 vaccinations india.
4. Doshi RH, Nsasiirwe S, Dahlke M, Atagbaza A, Aluta OE, Tatsinkou AB, Dauda E, Vilajeliu A, Gurung S, Tusiime J, Braka F, Bwaka A, Wanyoike S, Brooks DJ, Blanc DC, Alexander JPJ, Dahl BA, Lindstrand A, Wiysonge CS. 2024. COVID-19 Vaccination Coverage - World Health Organization African Region, 2021-2023. MMWR Morbidity and mortality weekly report 73:307–311.
5. Ministry of health and family welfare G of I. Ministry of Health and Family Welfare https://www.mohfw.gov.in Govt. Of India: COVID-19 data.
6. Sarkar A, Chakrabarti AK, Dutta S. 2021. Covid-19 Infection in India: A Comparative Analysis of the Second Wave with the First Wave. Pathogens https://doi.org/10.3390/pathogens10091222.
7. Tareq AM, Emran T Bin, Dhama K, Dhawan M, Tallei TE. 2021. Impact of SARS-CoV-2 delta variant (B.1.617.2) in surging second wave of COVID-19 and efficacy of vaccines in tackling the ongoing pandemic. Human Vaccines & Immunotherapeutics 17:4126–4127.
8. Chavda VP, Balar P, Vaghela D, Solanki HK, Vaishnav A, Hala V, Vora L. 2023. Omicron Variant of SARS-CoV-2: An Indian Perspective of Vaccination and Management. Vaccines https://doi.org/10.3390/vaccines11010160.
9. Krishna B, Gupta A, Meena K, Gaba A, Krishna S, Jyoti R, Aeron N, Prashanth S, Samriti, Ganapathy U. 2022. Prevalence, severity, and risk factor of breakthrough infection after vaccination with either the Covaxin or the Covishield among healthcare workers: A nationwide cross-sectional study. Journal of anaesthesiology, clinical pharmacology 38:S66–S78.
10. Kavitha C, Gowrisankar A, Banerjee S. 2021. The second and third waves in India: when will the pandemic be culminated? The European Physical Journal Plus 136:596.
11. Letko M, Marzi A, Munster V. 2020. Functional assessment of cell entry and receptor usage for SARS-CoV-2 and other lineage B betacoronaviruses. Nature microbiology 5:562–569.
12. Jackson CB, Farzan M, Chen B, Choe H. 2022. Mechanisms of SARS-CoV-2 entry into cells. Nature Reviews Molecular Cell Biology 23:3–20.
13. Xiaojie S, Yu L, lei Y, Guang Y, Min Q. 2021. Neutralizing antibodies targeting SARS-CoV-2 spike protein. Stem Cell Research 50:102125.
14. Xia S, Liu M, Wang C, Xu W, Lan Q, Feng S, Qi F, Bao L, Du L, Liu S, Qin C, Sun F, Shi Z, Zhu Y, Jiang S, Lu L. 2020. Inhibition of SARS-CoV-2 (previously 2019-nCoV) infection by a highly potent pan-coronavirus fusion inhibitor targeting its spike protein that harbors a high capacity to mediate membrane fusion. Cell Research 30:343–355.
15. Du L, He Y, Zhou Y, Liu S, Zheng B-J, Jiang S. 2009. The spike protein of SARS-CoV — a target for vaccine and therapeutic development. Nature Reviews Microbiology 7:226–236.
16. Wrapp D, Wang N, Corbett KS, Goldsmith JA, Hsieh CL, Abiona O, Graham BS, McLellan JS. 2020. Cryo-EM structure of the 2019-nCoV spike in the prefusion

720 conformation. Science 367:1260–1263.

721 17. Piccoli L, Park Y-J, Tortorici MA, Czudnochowski N, Walls AC, Beltramello M, Silacci-
722 Fregni C, Pinto D, Rosen LE, Bowen JE, Acton OJ, Jaconi S, Guarino B, Minola A,
723 Zatta F, Sprugasci N, Bassi J, Peter A, De Marco A, Nix JC, Mele F, Jovic S,
724 Rodriguez BF, Gupta S V, Jin F, Piumatti G, Lo Presti G, Pellanda AF, Biggiogero M,
725 Tarkowski M, Pizzuto MS, Cameroni E, Havenar-Daughton C, Smithey M, Hong D,
726 Lepori V, Albanese E, Ceschi A, Bernasconi E, Elzi L, Ferrari P, Garzoni C, Riva A,
727 Snell G, Sallusto F, Fink K, Virgin HW, Lanzavecchia A, Corti D, Veesler D. 2020.
728 Mapping Neutralizing and Immunodominant Sites on the SARS-CoV-2 Spike
729 Receptor-Binding Domain by Structure-Guided High-Resolution Serology. Cell
730 183:1024-1042.e21.

731 18. Steffen TL, Stone ET, Hassert M, Geerling E, Grimberg BT, Espino AM, Pantoja P,
732 Climent C, Hoft DF, George SL, Sariol CA, Pinto AK, Brien JD. 2020. The receptor
733 binding domain of SARS-CoV-2 spike is the key target of neutralizing antibody in
734 human polyclonal sera. bioRxiv 2020.08.21.261727.

735 19. Greaney AJ, Loes AN, Crawford KHD, Starr TN, Malone KD, Chu HY, Bloom JD.
736 2021. Comprehensive mapping of mutations in the SARS-CoV-2 receptor-binding
737 domain that affect recognition by polyclonal human plasma antibodies. Cell Host &
738 Microbe 29:463-476.e6.

739 20. Chen Y, Zhao X, Zhou H, Zhu H, Jiang S, Wang P. 2023. Broadly neutralizing
740 antibodies to SARS-CoV-2 and other human coronaviruses. Nature Reviews
741 Immunology 23:189–199.

742 21. Barnes CO, Jette CA, Abernathy ME, Dam K-MA, Esswein SR, Gristick HB, Malyutin
743 AG, Sharaf NG, Huey-Tubman KE, Lee YE, Robbiani DF, Nussenzweig MC, West AP,
744 Bjorkman PJ. 2020. SARS-CoV-2 neutralizing antibody structures inform therapeutic
745 strategies. Nature 588:682–687.

746 22. Pinto D, Park Y-J, Beltramello M, Walls AC, Tortorici MA, Bianchi S, Jaconi S, Culap
747 K, Zatta F, De Marco A, Peter A, Guarino B, Spreafico R, Cameroni E, Case JB, Chen
748 RE, Havenar-Daughton C, Snell G, Telenti A, Virgin HW, Lanzavecchia A, Diamond
749 MS, Fink K, Veesler D, Corti D. 2020. Cross-neutralization of SARS-CoV-2 by a
750 human monoclonal SARS-CoV antibody. Nature 583:290–295.

751 23. Yuan M, Wu NC, Zhu X, Lee C-CD, So RTY, Lv H, Mok CKP, Wilson IA. 2020. A highly
752 conserved cryptic epitope in the receptor binding domains of SARS-CoV-2 and SARS-
753 CoV. Science 368:630–633.

754 24. Huang Y, Yang C, Xu X feng, Xu W, Liu S wen. 2020. Structural and functional
755 properties of SARS-CoV-2 spike protein: potential antivirus drug development for
756 COVID-19. Acta Pharmacologica Sinica 41:1141–1149.

757 25. Liu H, Wu NC, Yuan M, Bangaru S, Torres JL, Caniels TG, van Schooten J, Zhu X,
758 Lee C-CD, Brouwer PJM, van Gils MJ, Sanders RW, Ward AB, Wilson IA. 2020.
759 Cross-Neutralization of a SARS-CoV-2 Antibody to a Functionally Conserved Site Is
760 Mediated by Avidity. Immunity 53:1272-1280.e5.

761 26. Jette CA, Cohen AA, Gnanapragasam PNP, Muecksch F, Lee YE, Huey-Tubman KE,
762 Schmidt F, Hatziioannou T, Bieniasz PD, Nussenzweig MC, West AP, Keeffe JR,
763 Bjorkman PJ, Barnes CO. 2021. Broad cross-reactivity across sarbecoviruses
764 exhibited by a subset of COVID-19 donor-derived neutralizing antibodies. Cell
765 Reports 36:109760.

766 27. Jensen JL, Sankhala RS, Dussupt V, Bai H, Hajduczki A, Lal KG, Chang WC,
767 Martinez EJ, Peterson CE, Golub ES, Rees PA, Mendez-Rivera L, Zemil M, Kavusak
768 E, Mayer S V, Wieczorek L, Kannan S, Doranz BJ, Davidson E, Yang ES, Zhang Y,
769 Chen M, Choe M, Wang L, Gromowski GD, Koup RA, Michael NL, Polonis VR,
770 Rolland M, Modjarrad K, Krebs SJ, Joyce MG. 2023. Targeting the Spike Receptor
771 Binding Domain Class V Cryptic Epitope by an Antibody with Pan-Sarbecovirus

772 Activity. Journal of virology 97:e0159622.

773 28. Rouet R, Henry JY, Johansen MD, Sobti M, Balachandran H, Langley DB, Walker GJ,
774 Lenthall H, Jackson J, Ubiparipovic S, Mazigi O, Schofield P, Burnett DL, Brown SHJ,
775 Martinello M, Hudson B, Gilroy N, Post JJ, Kelleher A, Jäck H-M, Goodnow CC,
776 Turville SG, Rawlinson WD, Bull RA, Stewart AG, Hansbro PM, Christ D. 2023.
777 Broadly neutralizing SARS-CoV-2 antibodies through epitope-based selection from
778 convalescent patients. Nature Communications 14:687.

779 29. Chandra S, Manjunath K, Asok A, Varadarajan R. 2023. Mutational scan inferred
780 binding energetics and structure in intrinsically disordered protein CcdA. Protein
781 science : a publication of the Protein Society 32:e4580.

782 30. Chandra S, Chattopadhyay G, Varadarajan R. 2021. Rapid Identification of Secondary
783 Structure and Binding Site Residues in an Intrinsically Disordered Protein Segment.
784 Frontiers in genetics 12:755292.

785 31. Rao X, Zhao R, Tong Z, Guo S, Peng W, Liu K, Li S, Wu L, Tong J, Chai Y, Han P,
786 Wang F, Jia P, Li Z, Zhao X, Li D, Zhang R, Zhang X, Zou W, Li W, Wang Q, Gao GF,
787 Wu Y, Dai L, Gao F. 2023. Defining a de novo non-RBM antibody as RBD-8 and its
788 synergistic rescue of immune-evaded antibodies to neutralize Omicron SARS-CoV-2.
789 Proceedings of the National Academy of Sciences 120:e2314193120.

790 32. Bates TA, McBride SK, Leier HC, Guzman G, Lyski ZL, Schoen D, Winders B, Lee J-
791 Y, Lee DX, Messer WB, Curlin ME, Tafesse FG. 2022. Vaccination before or after
792 SARS-CoV-2 infection leads to robust humoral response and antibodies that
793 effectively neutralize variants. Science immunology 7:eabn8014.

794 33. Walls AC, Sprouse KR, Bowen JE, Joshi A, Franko N, Navarro MJ, Stewart C,
795 Cameroni E, McCallum M, Goecker EA, Degli-Angeli EJ, Logue J, Greninger A, Corti
796 D, Chu HY, Veesler D. 2022. SARS-CoV-2 breakthrough infections elicit potent, broad,
797 and durable neutralizing antibody responses. Cell 185:872-880.e3.

798 34. Swami A, Mohanty A, Jamwal A, Turbadkar D, Baveja S, Shastri J, Chitalia V. 2023. A
799 comparative analysis of the second and third wave of the Covid-19 pandemic: an
800 experience from a tertiary care hospital in Western India. Journal of medical
801 microbiology 72.

802 35. Jana I Das, Bhattacharya P, Mayilsamy K, Banerjee S, Bhattacharje G, Das S, Aditya
803 S, Ghosh A, McGill AR, Srikrishnan S, Das AK, Basak A, Mohapatra SS, Chandran B,
804 Bhimsaria D, Mohapatra S, Roy A, Mondal A. 2022. Targeting an evolutionarily
805 conserved “e-L-L” motif in spike protein to identify a small molecule fusion inhibitor
806 against SARS-CoV-2. PNAS Nexus 1:1–14.

807 36. Malladi SK, Patel UR, Rajmani RS, Singh R, Pandey S, Kumar S, Khaleeq S, van
808 Vuren PJ, Riddell S, Goldie S, Gayathri S, Chakraborty D, Kalita P, Pramanick I,
809 Agarwal N, Reddy P, Girish N, Upadhyaya A, Khan MS, Kanjo K, Bhat M, Mani S,
810 Bhattacharyya S, Siddiqui S, Tyagi A, Jha S, Pandey R, Tripathi S, Dutta S, McAuley
811 AJ, Singanallur NB, Vasan SS, Ringe RP, Varadarajan R. 2021. Immunogenicity and
812 Protective Efficacy of a Highly Thermotolerant, Trimeric SARS-CoV-2 Receptor
813 Binding Domain Derivative. ACS infectious diseases 7:2546–2564.

814 37. Wenlin R, Xiaohui J, Mingli G, Jun L, Yanying Y, Quanxin L, J. KD, K. OA, Yu Z, Jin Z,
815 Guocai Z, Florian D, Xinquan W, Ailong H, Rong Z, Qiang D. 2022. Characterization
816 of SARS-CoV-2 Variants B.1.617.1 (Kappa), B.1.617.2 (Delta), and B.1.618 by Cell
817 Entry and Immune Evasion. mBio 13:e00099-22.

818 38. Servellita V, Syed AM, Morris MK, Brazer N, Saldhi P, Garcia-Knight M, Sreekumar B,
819 Khalid MM, Ciling A, Chen P-Y, Kumar GR, Gliwa AS, Nguyen J, Sotomayor-Gonzalez
820 A, Zhang Y, Frias E, Prostko J, Hackett J, Andino R, Wadford DA, Hanson C, Doudna
821 J, Ott M, Chiu CY. 2022. Neutralizing immunity in vaccine breakthrough infections
822 from the SARS-CoV-2 Omicron and Delta variants. Cell 185:1539-1548.e5.

823 39. Ai J, Zhang H, Zhang Y, Lin K, Zhang Y, Wu J, Wan Y, Huang Y, Song J, Fu Z, Wang

824 H, Guo J, Jiang N, Fan M, Zhou Y, Zhao Y, Zhang Q, Liu Q, Lv J, Li P, Qiu C, Zhang
825 W. 2022. Omicron variant showed lower neutralizing sensitivity than other SARS-CoV-
826 2 variants to immune sera elicited by vaccines after boost. Emerging Microbes &
827 Infections 11:337–343.

828 40. Greaney AJ, Starr TN, Barnes CO, Weisblum Y, Schmidt F, Caskey M, Gaebler C,
829 Cho A, Agudelo M, Finkin S, Wang Z, Poston D, Muecksch F, Hatziioannou T,
830 Bieniasz PD, Robbiani DF, Nussenzweig MC, Bjorkman PJ, Bloom JD. 2021. Mapping
831 mutations to the SARS-CoV-2 RBD that escape binding by different classes of
832 antibodies. Nature Communications 12:4196.

833 41. Wang Q, Iketani S, Li Z, Liu L, Guo Y, Huang Y, Bowen AD, Liu M, Wang M, Yu J,
834 Valdez R, Lauring AS, Sheng Z, Wang HH, Gordon A, Liu L, Ho DD. 2023. Alarming
835 antibody evasion properties of rising SARS-CoV-2 BQ and XBB subvariants. Cell
836 186:279-286.e8.

837 42. Kugathasan R, Sukhova K, Moshe M, Kellam P, Barclay W. 2023. Deep mutagenesis
838 scanning using whole trimeric SARS-CoV-2 spike highlights the importance of NTD-
839 RBD interactions in determining spike phenotype. PLoS pathogens 19:e1011545.

840 43. Greaney AJ, Eguia RT, Starr TN, Khan K, Franko N, Logue JK, Lord SM, Speake C,
841 Chu HY, Sigal A, Bloom JD. 2022. The SARS-CoV-2 Delta variant induces an
842 antibody response largely focused on class 1 and 2 antibody epitopes. PLOS
843 Pathogens 18:e1010592.

844 44. Tanaka S, Olson CA, Barnes CO, Higashide W, Gonzalez M, Taft J, Richardson A,
845 Martin-Fernandez M, Bogunovic D, Gnanapragasam PNP, Bjorkman PJ, Spilman P,
846 Niazi K, Rabizadeh S, Soon-Shiong P. 2022. Rapid identification of neutralizing
847 antibodies against SARS-CoV-2 variants by mRNA display. Cell Reports 38:110348.

848 45. Li T, Xue W, Zheng Q, Song S, Yang C, Xiong H, Zhang S, Hong M, Zhang Y, Yu H,
849 Zhang Y, Sun H, Huang Y, Deng T, Chi X, Li J, Wang S, Zhou L, Chen T, Wang Y,
850 Cheng T, Zhang T, Yuan Q, Zhao Q, Zhang J, McLellan JS, Zhou ZH, Zhang Z, Li S,
851 Gu Y, Xia N. 2021. Cross-neutralizing antibodies bind a SARS-CoV-2 cryptic site and
852 resist circulating variants. Nature Communications 12:5652.

853 46. Sankhala RS, Dussupt V, Chen W-H, Bai H, Martinez EJ, Jensen JL, Rees PA,
854 Hajduczki A, Chang WC, Choe M, Yan L, Sterling SL, Swafford I, Kuklis C, Soman S,
855 King J, Corbitt C, Zemil M, Peterson CE, Mendez-Rivera L, Townsley SM, Donofrio
856 GC, Lal KG, Tran U, Green EC, Smith C, de Val N, Laing ED, Broder CC, Currier JR,
857 Gromowski GD, Wieczorek L, Rolland M, Paquin-Proulx D, van Dyk D, Britton Z,
858 Rajan S, Loo YM, McTamney PM, Esser MT, Polonis VR, Michael NL, Krebs SJ,
859 Modjarrad K, Joyce MG. 2024. Antibody targeting of conserved sites of vulnerability
860 on the SARS-CoV-2 spike receptor-binding domain. Structure (London, England :
861 1993) 32:131-147.e7.

862 47. Starr TN, Czudnochowski N, Liu Z, Zatta F, Park Y-J, Addetia A, Pinto D, Beltramello
863 M, Hernandez P, Greaney AJ, Marzi R, Glass WG, Zhang I, Dingens AS, Bowen JE,
864 Tortorici MA, Walls AC, Wojcechowskyj JA, De Marco A, Rosen LE, Zhou J, Montiel-
865 Ruiz M, Kaiser H, Dillen JR, Tucker H, Bassi J, Silacci-Fregni C, Housley MP, di Iulio
866 J, Lombardo G, Agostini M, Sprugasci N, Culap K, Jaconi S, Meury M, Dellota Jr E,
867 Abdelnabi R, Foo S-YC, Cameroni E, Stumpf S, Croll TI, Nix JC, Havenar-Daughton
868 C, Piccoli L, Benigni F, Neyts J, Telenti A, Lempp FA, Pizzuto MS, Chodera JD,
869 Hebner CM, Virgin HW, Whelan SPJ, Veesler D, Corti D, Bloom JD, Snell G. 2021.
870 SARS-CoV-2 RBD antibodies that maximize breadth and resistance to escape.
871 Nature 597:97–102.

872 48. Hotez P. 2023. XBB.1.5 emerges in the Americas: what it means to the region. Lancet
873 regional health Americas 18:100433.

874 49. Callaway E. 2023. Coronavirus variant XBB.1.5 rises in the United States - is it a
875 global threat? Nature. England https://doi.org/10.1038/d41586-023-00014-3.

50. Ao D, He X, Hong W, Wei X. 2023. The rapid rise of SARS-CoV-2 Omicron subvariants with immune evasion properties: XBB.1.5 and BQ.1.1 subvariants. MedComm 4:e239.

51. Parums D V. 2023. Editorial: The XBB.1.5 ('Kraken') Subvariant of Omicron SARS-CoV-2 and its Rapid Global Spread. Medical science monitor : international medical journal of experimental and clinical research. United States https://doi.org/10.12659/MSM.939580.

52. Machado RRG, Candido ÉD, Aguiar AS, Chalup VN, Sanches PR, Dorlass EG, Amgarten DE, Pinho JRR, Durigon EL, Oliveira DBL. 2024. Immune Evasion of SARS-CoV-2 Omicron Subvariants XBB.1.5, XBB.1.16 and EG.5.1 in a Cohort of Older Adults after ChAdOx1-S Vaccination and BA.4/5 Bivalent Booster. Vaccines 12.

53. Chen J-J, Li L-B, Peng H-H, Tian S, Ji B, Shi C, Qian C, Jiang W-G, Liu M-C, Li T-T, Shen Y, Fang L-Q, Wang G-L. 2023. Neutralization against XBB.1 and XBB.1.5 after omicron subvariants breakthrough infection or reinfection. The Lancet regional health Western Pacific 33:100759.

54. Cao Y, Jian F, Wang J, Yu Y, Song W, Yisimayi A, Wang J, An R, Chen X, Zhang N, Wang Y, Wang P, Zhao L, Sun H, Yu L, Yang S, Niu X, Xiao T, Gu Q, Shao F, Hao X, Xu Y, Jin R, Shen Z, Wang Y, Xie XS. 2023. Imprinted SARS-CoV-2 humoral immunity induces convergent Omicron RBD evolution. Nature 614:521–529.

55. Jian F, Feng L, Yang S, Yu Y, Wang L, Song W, Yisimayi A, Chen X, Xu Y, Wang P, Yu L, Wang J, Liu L, Niu X, Wang J, Xiao T, An R, Wang Y, Gu Q, Shao F, Jin R, Shen Z, Wang Y, Wang X, Cao Y. 2023. Convergent evolution of SARS-CoV-2 XBB lineages on receptor-binding domain 455-456 synergistically enhances antibody evasion and ACE2 binding. PLoS pathogens 19:e1011868.

56. Kitchin D, Richardson SI, van der Mescht MA, Motlou T, Mzindle N, Moyo-Gwete T, Makhado Z, Ayres F, Manamela NP, Spencer H, Lambson B, Oosthuysen B, Kaldine H, du Pisanie M, Mennen M, Skelem S, Williams N, Ntusi NAB, Burgers WA, Gray GG, Bekker L-G, Boswell MT, Rossouw TM, Ueckermann V, Moore PL. 2022. Ad26.COV2.S breakthrough infections induce high titers of neutralizing antibodies against Omicron and other SARS-CoV-2 variants of concern. Cell Reports Medicine 3:100535.

57. Nutalai R, Zhou D, Tuekprakhon A, Ginn HM, Supasa P, Liu C, Huo J, Mentzer AJ, Duyvesteyn HME, Dijokaite-Guraliuc A, Skelly D, Ritter TG, Amini A, Bibi S, Adele S, Johnson SA, Constantinides B, Webster H, Temperton N, Klenerman P, Barnes E, Dunachie SJ, Crook D, Pollard AJ, Lambe T, Goulder P, Paterson NG, Williams MA, Hall DR, Mongkolsapaya J, Fry EE, Dejnirattisai W, Ren J, Stuart DI, Screaton GR. 2022. Potent cross-reactive antibodies following Omicron breakthrough in vaccinees. Cell 185:2116-2131.e18.

58. Lapuente D, Winkler TH, Tenbusch M. 2024. B-cell and antibody responses to SARS-CoV-2: infection, vaccination, and hybrid immunity. Cellular & molecular immunology 21:144–158.

59. Andreano E, Paciello I, Pierleoni G, Maccari G, Antonelli G, Abbiento V, Pileri P, Benincasa L, Giglioli G, Piccini G, De Santi C, Sala C, Medini D, Montomoli E, Maes P, Rappuoli R. 2023. mRNA vaccines and hybrid immunity use different B cell germlines against Omicron BA.4 and BA.5. Nature communications 14:1734.

60. Andreano E, Paciello I, Piccini G, Manganaro N, Pileri P, Hyseni I, Leonardi M, Pantano E, Abbiento V, Benincasa L, Giglioli G, De Santi C, Fabbiani M, Rancan I, Tumbarello M, Montagnani F, Sala C, Montomoli E, Rappuoli R. 2021. Hybrid immunity improves B cells and antibodies against SARS-CoV-2 variants. Nature 600:530–535.

61. Tas JMJ, Koo J-H, Lin Y-C, Xie Z, Steichen JM, Jackson AM, Hauser BM, Wang X, Cottrell CA, Torres JL, Warner JE, Kirsch KH, Weldon SR, Groschel B, Nogal B,

928 Ozorowski G, Bangaru S, Phelps N, Adachi Y, Eskandarzadeh S, Kubitz M, Burton
929 DR, Lingwood D, Schmidt AG, Nair U, Ward AB, Schief WR, Batista FD. 2022.
930 Antibodies from primary humoral responses modulate the recruitment of naive B cells
931 during secondary responses. Immunity 55:1856-1871.e6.

932 62. Wratil PR, Stern M, Priller A, Willmann A, Almanzar G, Vogel E, Feuerherd M, Cheng
933 C-C, Yazici S, Christa C, Jeske S, Lupoli G, Vogt T, Albanese M, Mejías-Pérez E,
934 Bauernfried S, Graf N, Mijocevic H, Vu M, Tinnefeld K, Wettengel J, Hoffmann D,
935 Muenchhoff M, Daechert C, Mairhofer H, Krebs S, Fingerle V, Graf A, Steininger P,
936 Blum H, Hornung V, Liebl B, Überla K, Prelog M, Knolle P, Keppler OT, Protzer U.
937 2022. Three exposures to the spike protein of SARS-CoV-2 by either infection or
938 vaccination elicit superior neutralizing immunity to all variants of concern. Nature
939 medicine 28:496–503.

940 63. Miyamoto S, Arashiro T, Adachi Y, Moriyama S, Kinoshita H, Kanno T, Saito S, Katano
941 H, Iida S, Ainai A, Kotaki R, Yamada S, Kuroda Y, Yamamoto T, Ishijima K, Park E-S,
942 Inoue Y, Kaku Y, Tobiume M, Iwata-Yoshikawa N, Shiwa-Sudo N, Tokunaga K, Ozono
943 S, Hemmi T, Ueno A, Kishida N, Watanabe S, Nojima K, Seki Y, Mizukami T,
944 Hasegawa H, Ebihara H, Maeda K, Fukushi S, Takahashi Y, Suzuki T. 2022.
945 Vaccination-infection interval determines cross-neutralization potency to SARS-CoV-2
946 Omicron after breakthrough infection by other variants. Med (New York, NY) 3:249-
947 261.e4.

948 64. Park Y-J, Pinto D, Walls AC, Liu Z, Marco A De, Benigni F, Zatta F, Silacci-Fregni C,
949 Bassi J, Sprouse KR, Addetia A, Bowen JE, Stewart C, Giurdanella M, Saliba C,
950 Guarino B, Schmid MA, Franko N, Logue J, Dang H V, Hauser K, Iulio J di, Rivera W,
951 Schnell G, Rajesh A, Zhou J, Farhat N, Kaiser H, Montiel-Ruiz M, Noack J, Lempp
952 FA, Janer J, Abdelnabi R, Maes P, Ferrari P, Ceschi A, Giannini O, de Melo GD,
953 Kergoat L, Bourhy H, Neyts J, Soriaga L, Purcell LA, Snell G, Whelan SPJ,
954 Lanzavecchia A, Virgin HW, Piccoli L, Chu H, Pizzuto MS, Corti D, Veesler D. 2022.
955 Imprinted antibody responses against SARS-CoV-2 Omicron sublineages. bioRxiv :
956 the preprint server for biology. United States
957 https://doi.org/10.1101/2022.05.08.491108.

958 65. Quandt J, Muik A, Salisch N, Lui BG, Lutz S, Krüger K, Wallisch A-K, Adams-Quack P,
959 Bacher M, Finlayson A, Ozhelvaci O, Vogler I, Grikscheit K, Hoehl S, Goetsch U,
960 Ciesek S, Türeci Ö, Sahin U. 2022. Omicron BA.1 breakthrough infection drives
961 cross-variant neutralization and memory B cell formation against conserved epitopes.
962 Science immunology 7:eabq2427.

963 66. Greaney AJ, Starr TN, Gilchuk P, Zost SJ, Binshtein E, Loes AN, Hilton SK,
964 Huddleston J, Eguia R, Crawford KHD, Dingens AS, Nargi RS, Sutton RE,
965 Suryadevara N, Rothlauf PW, Liu Z, Whelan SPJ, Carnahan RH, Crowe JEJ, Bloom
966 JD. 2021. Complete Mapping of Mutations to the SARS-CoV-2 Spike Receptor-
967 Binding Domain that Escape Antibody Recognition. Cell host & microbe 29:44-57.e9.

968 67. Greaney AJ, Loes AN, Gentles LE, Crawford KHD, Starr TN, Malone KD, Chu HY,
969 Bloom JD. 2021. Antibodies elicited by mRNA-1273 vaccination bind more broadly to
970 the receptor binding domain than do those from SARS-CoV-2 infection. Science
971 translational medicine 13.

972 68. Cao Y, Yisimayi A, Jian F, Song W, Xiao T, Wang L, Du S, Wang J, Li Q, Chen X, Yu Y,
973 Wang P, Zhang Z, Liu P, An R, Hao X, Wang Y, Wang J, Feng R, Sun H, Zhao L,
974 Zhang W, Zhao D, Zheng J, Yu L, Li C, Zhang N, Wang R, Niu X, Yang S, Song X,
975 Chai Y, Hu Y, Shi Y, Zheng L, Li Z, Gu Q, Shao F, Huang W, Jin R, Shen Z, Wang Y,
976 Wang X, Xiao J, Xie XS. 2022. BA.2.12.1, BA.4 and BA.5 escape antibodies elicited
977 by Omicron infection. Nature 608:593–602.

978 69. Cao Y, Wang J, Jian F, Xiao T, Song W, Yisimayi A, Huang W, Li Q, Wang P, An R,
979 Wang J, Wang Y, Niu X, Yang S, Liang H, Sun H, Li T, Yu Y, Cui Q, Liu S, Yang X, Du
980 S, Zhang Z, Hao X, Shao F, Jin R, Wang X, Xiao J, Wang Y, Xie XS. 2022. Omicron

981 escapes the majority of existing SARS-CoV-2 neutralizing antibodies. Nature
982 602:657–663.

983 70. Carr EJ, Wu MY, Gahir J, Harvey R, Townsley H, Bailey C, Fowler AS, Dowgier G,
984 Hobbs A, Herman L, Ragno M, Miah M, Bawumia P, Smith C, Miranda M, Mears H V,
985 Adams L, Haptipoglu E, O'Reilly N, Warchal S, Sawyer C, Ambrose K, Kelly G, Beale
986 R, Papineni P, Corrah T, Gilson R, Gamblin S, Kassiotis G, Libri V, Williams B,
987 Swanton C, Gandhi S, Lv Bauer D, Wall EC. 2023. Neutralising immunity to omicron
988 sublineages BQ.1.1, XBB, and XBB.1.5 in healthy adults is boosted by bivalent BA.1-
989 containing mRNA vaccination and previous Omicron infection. The Lancet Infectious
990 diseases. United States https://doi.org/10.1016/S1473-3099(23)00289-X.

991 71. Nham E, Kim J, Lee J, Park H, Kim J, Lee S, Choi J, Kim KT, Yoon JG, Hwang SY,
992 Song JY, Cheong HJ, Kim WJ, Park M-S, Noh JY. 2023. Low Neutralizing Activities to
993 the Omicron Subvariants BN.1 and XBB.1.5 of Sera From the Individuals Vaccinated
994 With a BA.4/5-Containing Bivalent mRNA Vaccine. Immune network 23:e43.

995 72. Qian Wang , Yicheng Guo , Anthony Bowen , Ian A Mellis , Riccardo Valdez , Carmen
996 Gherasim , Abree Gordon , Lihong Liu DDH. 2024. XBB.1.5 monovalent mRNA
997 vaccine booster elicits robust neutralizing antibodies against XBB subvariants and
998 JN.1. Cell host & microbe 32:315-321.e3.

999 73. Miller J, Hachmann NP, Collier A-RY, Lasrado N, Mazurek CR, Patio RC, Powers O,
1000 Surve N, Theiler J, Korber B, Barouch DH. 2023. Substantial Neutralization Escape by
1001 SARS-CoV-2 Omicron Variants BQ.1.1 and XBB.1. The New England journal of
1002 medicine. United States https://doi.org/10.1056/NEJMc2214314.

1003 74. Raksha D, Rohini D, Raghavan V. 2020. Probing the Structure of the HIV-1 Envelope
1004 Trimer Using Aspartate Scanning Mutagenesis. Journal of Virology
1005 94:10.1128/jvi.01426-20.

1006 75. Bajaj K, Chakrabarti P, Varadarajan R. 2005. Mutagenesis-based definitions and
1007 probes of residue burial in proteins. Proceedings of the National Academy of Sciences
1008 102:16221–16226.

1009 76. Rappazzo CG, Tse L V, Kaku CI, Wrapp D, Sakharkar M, Huang D, Deveau LM,
1010 Yockachonis TJ, Herbert AS, Battles MB, O'Brien CM, Brown ME, Geoghegan JC,
1011 Belk J, Peng L, Yang L, Hou Y, Scobey TD, Burton DR, Nemazee D, Dye JM, Voss
1012 JE, Gunn BM, McLellan JS, Baric RS, Gralinski LE, Walker LM. 2021. Broad and
1013 potent activity against SARS-like viruses by an engineered human monoclonal
1014 antibody. Science (New York, NY) 371:823–829.

1015 77. Joseph J, Darpe S, Kulkarni G, Raj VS. 2023. SARS-CoV-2 neutralizing antibody
1016 epitopes are overlapping and highly mutated which raises the chances of escape
1017 variants and requires development of broadly reactive vaccines. Proteins 91:1021–
1018 1031.

1019 78. Dejnirattisai W, Zhou D, Ginn HM, Duyvesteyn HME, Supasa P, Case JB, Zhao Y,
1020 Walter TS, Mentzer AJ, Liu C, Wang B, Paesen GC, Slon-Campos J, López-Camacho
1021 C, Kafai NM, Bailey AL, Chen RE, Ying B, Thompson C, Bolton J, Fyfe A, Gupta S,
1022 Tan TK, Gilbert-Jaramillo J, James W, Knight M, Carroll MW, Skelly D, Dold C, Peng
1023 Y, Levin R, Dong T, Pollard AJ, Knight JC, Klenerman P, Temperton N, Hall DR,
1024 Williams MA, Paterson NG, Bertram FKR, Siebert CA, Clare DK, Howe A, Radecke J,
1025 Song Y, Townsend AR, Huang K-YA, Fry EE, Mongkolsapaya J, Diamond MS, Ren J,
1026 Stuart DI, Screaton GR. 2021. The antigenic anatomy of SARS-CoV-2 receptor
1027 binding domain. Cell 184:2183-2200.e22.

1028 79. Huang K-YA, Tan TK, Chen T-H, Huang C-G, Harvey R, Hussain S, Chen C-P,
1029 Harding A, Gilbert-Jaramillo J, Liu X, Knight M, Schimanski L, Shih S-R, Lin Y-C,
1030 Cheng C-Y, Cheng S-H, Huang Y-C, Lin T-Y, Jan J-T, Ma C, James W, Daniels RS,
1031 McCauley JW, Rijal P, Townsend AR. 2021. Correction: Breadth and function of
1032 antibody response to acute SARS-CoV-2 infection in humans. PLOS Pathogens

1033 17:e1010148.

1034 80. Tortorici MA, Beltramello M, Lempp FA, Pinto D, Dang H V, Rosen LE, McCallum M,
1035 Bowen J, Minola A, Jaconi S, Zatta F, De Marco A, Guarino B, Bianchi S, Lauron EJ,
1036 Tucker H, Zhou J, Peter A, Havenar-Daughton C, Wojcechowskyj JA, Case JB, Chen
1037 RE, Kaiser H, Montiel-Ruiz M, Meury M, Czudnochowski N, Spreafico R, Dillen J, Ng
1038 C, Sprugasci N, Culap K, Benigni F, Abdelnabi R, Foo S-YC, Schmid MA, Cameroni
1039 E, Riva A, Gabrieli A, Galli M, Pizzuto MS, Neyts J, Diamond MS, Virgin HW, Snell G,
1040 Corti D, Fink K, Veesler D. 2020. Ultrapotent human antibodies protect against SARS-
1041 CoV-2 challenge via multiple mechanisms. Science 370:950–957.

1042 81. Tortorici MA, Czudnochowski N, Starr TN, Marzi R, Walls AC, Zatta F, Bowen JE,
1043 Jaconi S, Di Iulio J, Wang Z, De Marco A, Zepeda SK, Pinto D, Liu Z, Beltramello M,
1044 Bartha I, Housley MP, Lempp FA, Rosen LE, Dellota E, Kaiser H, Montiel-Ruiz M,
1045 Zhou J, Addetia A, Guarino B, Culap K, Sprugasci N, Saliba C, Vetti E, Giacchetto-
1046 Sasselli I, Fregni CS, Abdelnabi R, Foo S-YC, Havenar-Daughton C, Schmid MA,
1047 Benigni F, Cameroni E, Neyts J, Telenti A, Virgin HW, Whelan SPJ, Snell G, Bloom
1048 JD, Corti D, Veesler D, Pizzuto MS. 2021. Broad sarbecovirus neutralization by a
1049 human monoclonal antibody. Nature 597:103–108.

1050 82. Wang R, Chen J, Gao K, Wei G-W. 2021. Vaccine-escape and fast-growing mutations
1051 in the United Kingdom, the United States, Singapore, Spain, India, and other COVID-
1052 19-devastated countries. Genomics 113:2158–2170.

1053 83. Veronika T, Hemantha K, Lydia L, Victoria B, Elena R, Dagmara K, Yulia S, Debarati
1054 C, Iryna M, Kai D, Kirthi K, Hao G, Curtis F, Dina G, James R, Mansour S, Evgeni S.
1055 2021. Acquisition of the L452R Mutation in the ACE2-Binding Interface of Spike
1056 Protein Triggers Recent Massive Expansion of SARS-CoV-2 Variants. Journal of
1057 Clinical Microbiology 59:10.1128/jcm.00921-21.

1058 84. Kurhade C, Zou J, Xia H, Liu M, Chang HC, Ren P, Xie X, Shi P. 2023. Low
1059 neutralization of SARS-CoV-2 Omicron BA.2.75.2, BQ.1.1 and XBB.1 by parental
1060 mRNA vaccine or a BA.5 bivalent booster. Nature Medicine 29:344–347.

1061 85. Parums D V. 2023. Editorial: A Rapid Global Increase in COVID-19 is Due to the
1062 Emergence of the EG.5 (Eris) Subvariant of Omicron SARS-CoV-2. Medical science
1063 monitor : international medical journal of experimental and clinical research. United
1064 States https://doi.org/10.12659/MSM.942244.

1065 86. Vellas C, Trémeaux P, Del Bello A, Latour J, Jeanne N, Ranger N, Danet C, Martin-
1066 Blondel G, Delobel P, Kamar N, Izopet J. 2022. Resistance mutations in SARS-CoV-2
1067 omicron variant in patients treated with sotrovimab. Clinical Microbiology and Infection
1068 28:1297–1299.

1069 87. Xiong H, Sun H, Wang S, Yuan L, Liu L, Zhu Y, Zhang J, Huang Y, Qi R, Jiang Y, Ma
1070 J, Zhou M, Ma Y, Fu R, Yan S, Yue M, Wu Y, Wei M, Wang Y, Li T, Wang Y, Zheng Z,
1071 Yu H, Cheng T, Li S, Yuan Q, Zhang J, Guan Y, Zheng Q, Zhang T, Xia N. 2022. The
1072 neutralizing breadth of antibodies targeting diverse conserved epitopes between
1073 SARS-CoV and SARS-CoV-2. Proceedings of the National Academy of Sciences
1074 119:e2204256119.

1075 88. Starr TN, Greaney AJ, Dingens AS, Bloom JD. 2021. Complete map of SARS-CoV-2
1076 RBD mutations that escape the monoclonal antibody LY-CoV555 and its cocktail with
1077 LY-CoV016. Cell Reports Medicine 2:100255.

1078 89. Hastie KM, Li H, Bedinger D, Schendel SL, Dennison SM, Li K, Rayaprolu V, Yu X,
1079 Mann C, Zandonatti M, Diaz Avalos R, Zyla D, Buck T, Hui S, Shaffer K, Hariharan C,
1080 Yin J, Olmedillas E, Enriquez A, Parekh D, Abraha M, Feeney E, Horn GQ, team1 C-
1081 D, Aldon Y, Ali H, Aracic S, Cobb RR, Federman RS, Fernandez JM, Glanville J,
1082 Green R, Grigoryan G, Lujan Hernandez AG, Ho DD, Huang K-YA, Ingraham J, Jiang
1083 W, Kellam P, Kim C, Kim M, Kim HM, Kong C, Krebs SJ, Lan F, Lang G, Lee S, Leung
1084 CL, Liu J, Lu Y, MacCamy A, McGuire AT, Palser AL, Rabbitts TH, Rikhtegaran

Tehrani Z, Sajadi MM, Sanders RW, Sato AK, Schweizer L, Seo J, Shen B, Snitselaar JL, Stamatatos L, Tan Y, Tomic MT, van Gils MJ, Youssef S, Yu J, Yuan TZ, Zhang Q, Peters B, Tomaras GD, Germann T, Saphire EO. 2021. Defining variant-resistant epitopes targeted by SARS-CoV-2 antibodies: A global consortium study. Science 374:472–478.

90. Martinez DR, Schäfer A, Gobeil S, Li D, De la Cruz G, Parks R, Lu X, Barr M, Stalls V, Janowska K, Beaudoin E, Manne K, Mansouri K, Edwards RJ, Cronin K, Yount B, Anasti K, Montgomery SA, Tang J, Golding H, Shen S, Zhou T, Kwong PD, Graham BS, Mascola JR, Montefiori DC, Alam SM, Sempowski GD, Khurana S, Wiehe K, Saunders KO, Acharya P, Haynes BF, Baric RS. 2024. A broadly cross-reactive antibody neutralizes and protects against sarbecovirus challenge in mice. Science Translational Medicine 14:eabj7125.

91. Cho H, Gonzales-Wartz KK, Huang D, Yuan M, Peterson M, Liang J, Beutler N, Torres JL, Cong Y, Postnikova E, Bangaru S, Talana CA, Shi W, Yang ES, Zhang Y, Leung K, Wang L, Peng L, Skinner J, Li S, Wu NC, Liu H, Dacon C, Moyer T, Cohen M, Zhao M, Lee FE-H, Weinberg RS, Douagi I, Gross R, Schmaljohn C, Pegu A, Mascola JR, Holbrook M, Nemazee D, Rogers TF, Ward AB, Wilson IA, Crompton PD, Tan J. 2024. Bispecific antibodies targeting distinct regions of the spike protein potently neutralize SARS-CoV-2 variants of concern. Science Translational Medicine 13:eabj5413.

92. Crawford KHD, Eguia R, Dingens AS, Loes AN, Malone KD, Wolf CR, Chu HY, Tortorici MA, Veesler D, Murphy M, Pettie D, King NP, Balazs AB, Bloom JD. 2020. Protocol and reagents for pseudotyping lentiviral particles with SARS-CoV-2 spike protein for neutralization assays. Viruses 12.

93. Li T, Cai H, Zhao Y, Li Y, Lai Y, Yao H, Liu LD, Sun Z, van Vlissingen MF, Kuiken T, GeurtsvanKessel CH, Zhang N, Zhou B, Lu L, Gong Y, Qin W, Mondal M, Duan B, Xu S, Richard AS, Raoul H, Chen J, Xu C, Wu L, Zhou H, Huang Z, Zhang X, Li J, Wang Y, Bi Y, Rockx B, Chen J, Meng F-L, Lavillette D, Li D. 2021. Uncovering a conserved vulnerability site in SARS-CoV-2 by a human antibody. EMBO molecular medicine 13:e14544.

94. Bullen G, Galson JD, Hall G, Villar P, Moreels L, Ledsgaard L, Mattiuzzo G, Bentley EM, Masters EW, Tang D, Millett S, Tongue D, Brown R, Diamantopoulos I, Parthiban K, Tebbutt C, Leah R, Chaitanya K, Ergueta-Carballo S, Pazeraitis D, Surade SB, Ashiru O, Crippa L, Cowan R, Bowler MW, Campbell JI, Lee W-YJ, Carr MD, Matthews D, Pfeffer P, Hufton SE, Sawmynaden K, Osbourn J, McCafferty J, Karatt-Vellatt A. 2021. Cross-Reactive SARS-CoV-2 Neutralizing Antibodies From Deep Mining of Early Patient Responses. Frontiers in immunology 12:678570.

95. Wu NC, Yuan M, Bangaru S, Huang D, Zhu X, Lee C-CD, Turner HL, Peng L, Yang L, Burton DR, Nemazee D, Ward AB, Wilson IA. 2020. A natural mutation between SARS-CoV-2 and SARS-CoV determines neutralization by a cross-reactive antibody. PLOS Pathogens 16:e1009089.

96. Barnes CO, West APJ, Huey-Tubman KE, Hoffmann MAG, Sharaf NG, Hoffman PR, Koranda N, Gristick HB, Gaebler C, Muecksch F, Lorenzi JCC, Finkin S, Hägglöf T, Hurley A, Millard KG, Weisblum Y, Schmidt F, Hatziioannou T, Bieniasz PD, Caskey M, Robbiani DF, Nussenzweig MC, Bjorkman PJ. 2020. Structures of Human Antibodies Bound to SARS-CoV-2 Spike Reveal Common Epitopes and Recurrent Features of Antibodies. Cell 182:828-842.e16.

Tables

Table 1. MFI ratios for the potential epitope residues

1138

Sl No.	Residue	MFI-expression/ MFI-binding		
		BCRTH-01	INK-09	INK-36
1	351	1.295788	1.273718	1.157062
2	355	1.219729	1.239262	1.197349
3	356	1.17089	-	-
4	359	-	-	1.081459
5	364	1.182295	-	-
6	380	-	1.148814	1.077429
7	381	1.260786	-	-
8	387	1.230637	-	-
9	403	1.292267	1.172926	1.120017
10	416	1.329536	1.175896	1.101252
11	420	1.163761	-	1.072276
12	421	1.218064	1.168982	1.115263
13	424	-	1.192174	1.081695
14	430	1.270088	-	-
15	437	1.301646	1.107961	1.117455
16	452	-	-	1.076026
17	456	1.185845	1.252503	1.192579
18	457	1.225249	1.222689	-
19	464	1.246659	1.128143	1.087599
20	465	1.225858	-	1.080284
21	466	1.341557	1.187018	1.116536
22	467	1.242733	1.221766	1.118558
23	470	1.178698	-	1.063863
24	473	1.169721	1.145745	1.100281
25	475	-	-	1.102217
26	489	-	1.234014	1.144957

1139
1140
1141
1142 **Table 2. Classification of epitopes.**
1143

Residue No.	Epitopes for serum samples			Epitope class	Antibody	Reference
	BCRTH -01	INK -09	INK -36			
351	+	+	+	Class 5/ RBD8	N-612-056; BIOLS56/ IMCAS74/ WRAIR-2057/ WRAIR-2134	(31, 44–46)
355	+	+	+	Class 5/ RBD8	N-612-056/ BIOLS56/ IMCAS74/ WRAIR-2063/ S2H97/ FD20/WRAIR-2057/WRAIR-2134	(27, 31, 44–46, 93, 94)
356	+	-	-	Class3/ Class 5/ RBD8	S309/	(22, 31, 44, 46)

					N-612-056/ IMCAS74/ WRAIR-2134	
359	-	-	+	Class3	S309	(22)
364	+	-	-	Unclassified	-	-
380	-	+	+	Class4	COVA1-16, CR3022	(25, 95)
381	+	-	-	Class4	COVA1-16, CR3022	(25, 95)
387	+	-	-	Unclassified		-
403	+	+	+	Class1	C002, C102, C121	(21)
416	+	+	+	Class1/ Class4	C105, COVA1-16, C118, C022,	(25, 26, 96)
420	+	-	+	Class1	C105, LY-CoV-016	(40, 88, 96)
421	+	+	+	Class1	C102	(21)
424	-	+	+	Class 5/ RBD8	BIOLS56/ IMCAS74/ WRAIR-2057/ WRAIR-2134	(31, 46)
430	+	-	-	Class4/ Class 5/ RBD8	C022/ BIOLS56/ IMCAS74/ WRAIR-2057/ WRAIR-2134	(26, 31, 46)
437	+	+	+	Class 4	C118	(26)
452	-	-	+	Class2	C144, C002	(21)
456	+	+	+	Class1	C002, C102, C121	(21)
457	+	+	-	Class 5	N-612-056, 6D6; WRAIR-2057/WRAIR-2134	(44, 46)
464	+	+	+	Class 5/ RBD8	N-612-056/ 6D6 & 7D6/ BIOLS56/ IMCAS74/ WRAIR-2063/ S2H97/ WRAIR-2057/ WRAIR-2134	(27, 31, 44–46, 93, 94)
465	+	-	+	Class 5/ RBD8	N-612-056/ 6D6 & 7D6/ BIOLS56/ IMCAS74/ WRAIR-2063/ S2H97/ WRAIR-2057/ WRAIR-2134	(27, 31, 44–46, 94)
466	+	+	+	Class 5/ RBD8	N-612-056/ 6D6 & 7D6/ BIOLS56/ IMCAS74/ WRAIR-2063/ S2H97/ WRAIR-2057/ WRAIR-2134	(31, 44, 45)
467	+	+	+	Class 5/ RBD8	N-612-056; IMCAS74/ WRAIR-2063/ S2H97/ WRAIR-2057/ WRAIR-2134	(31, 44)
470	+	-	+	Class2/ Class 5/ RBD8	C144/ 7D6, 6D6/ WRAIR-2057	(21, 45)
473	+	+	+	Class1	C102	(21)
475	-	-	+	Class1	C102	(21)
489	-	+	+	Class1	C102	(21)

Figure Legends

FIG 1. Study cohort and timeline. (A) Schematic representation of study design. (B) Distribution of the study cohort as a function of the timeline of vaccination and breakthrough infection in the context of the second and third wave of pandemics caused by different VOCs of SARS-CoV-2. Red bars indicate the time points of serum sample collection for the entire cohort (early) and subsequently for the selected individuals (late). (C) Age distribution of male and female volunteers included in the study cohort.

FIG 2. Neutralizing activity of the polyclonal serum samples isolated from the study cohort. (A) Heatmap of neutralizing activity of the 164 serum samples (at dilutions; 0.01, 0.001, 0.001) against the parental strain and different VOCs of SARS-CoV-2 with green to red representing the lowest to highest extent of neutralization (%). (B) Comparison of the relative neuralization efficacies of the serum samples (at 0.01 dilution) against parental strain and different VOCs. (C) Venn diagram showing cross-reactivity of the selected serum samples displaying more than 65% neutralization (at 0.01 dilution) towards at least one of the pseudoviral variants tested in this study. A total of 29 serum samples with >65% cross-reactivity towards all the VOCs tested in this study were designated as broadly cross-reactive sera (red diamonds in A). Each image shown here are a representative of three independent experiments performed in triplicates.

FIG 3. Comparative neutralizing activities of the selected serum samples collected at early and late time points. (A) Comparative analysis of the neutralization titers (IC_{50}) of serum samples isolated from the selected 9 volunteers during 1st (early) and second (late) batches of sample collection, against WA.1, B.1.617.2 and BA.1. (B) Heatmap showing fold change in the IC_{50} values for B.1.617.2 and BA.1 with respect to the parental WA.1 strain with red to white indicating higher to lower neutralization titers. (C) Comparative analysis of the pseudovirus neutralization titers of the serum samples isolated at early and late time points. (D) Heatmap representing variant-specific fold change in IC_{50} values. All data shown are averages of the results of at least three independent experiments ± SD.

FIG 4. **The serum samples show high binding affinity towards spike RBD**. (A) ELISA was performed to determine the binding affinity of the polyclonal serum samples towards spike RBD derived from WA.1 and Omicron subvariants BA.1 and BA.5. (B) Comparison of binding affinity of different serum samples (presented in the form of IC50) towards different RBD variants. (C) Fold change in IC50 values for the BA.1 and BA.5 variants with respect to the WA.1. Each data shown is a representative of at least three experiments performed independently.

FIG 5. Identification and validation of RBD epitope residues through yeast display analysis. (A) Schematic representation of the yeast display screening as described in the text. (B) The heat map represents the ratio of MFI-expression to MFI-binding extracted from deep sequencing reads analysis. The higher to lower ratios are represented in a red to blue gradient. The higher the ratio (*Red*), the more sera escape at that position. (C) The MFI-expression/ MFI-binding ratios are mapped on the RBD structure (PDB ID: 6M0J) following the same color scheme. The RBM is demarcated on the structure using a black line. (D) Validation was carried out using FACS by quantifying the binding of WT and the mutant RBDs, harboring mutations at the epitope and non-epitope residues, to BCRTH-01, INK09 and INK36 serum samples. The MFI-binding of WT and mutant RBDs w.r.t to the three serum samples are presented. Each image is a representative of two independent experiments performed in triplicates.

FIG 6. Epitope classification and characterization. (A) Individual epitope residues, as identified for the BCRTH01, INK09 and INK36 serum samples, are mapped on the surface of the RBD (PDB ID: 6M0J) and are color-coded based on the previously published epitope classes. (B) Class 5/ RBD8 epitopes identified in this study are mapped on the pre-fusion trimeric structure of the spike in its closed (PDB ID: 6VXX) and open (PDB ID: 6VYB) conformations. (C) Matrix representing the conservation of identified epitope residues across all major SARS-CoV-2 variants. Mutations of a specific residue in a particular variant are represented in red square. Epitope classes are designated using coloured diamonds.

FIG 7. Neutralisation titers (IC50) for WT and mutant pseudoviruses w.r.t selected serum samples. (A) Neutralisation curves for pseudoviruses with WT (WA.1) or mutant spike proteins, harbouring specific mutations at the epitope residues, with serial dilutions of the BCRTH-01, INK-09 and INK-36 sera as indicated. (B) Neutralisation titers (IC50) for WT and mutant pseudoviruses for three sera samples as indicated.

FIG 8. A considerable fraction of the study cohort shows neutralization activity against Omicron XBB.1.5. (A) Neutralisation curves for WA.1, BA. 1 and XBB. 1.5 pseudoviruses with serial dilutions of BCRTH-01, INK-09 and INK 36 sera. (B) Neutralisation titers (IC50) of 29 serum samples (from FIG. 2C) w.r.t WA.1 and XBB.1.5 pseudoviruses are plotted. Fold change of the IC50 for XBB.1.5 w.r.t the WA.1 are marked in salmon red. All data shown are averages of the results of at least three independent experiments ± SD. $*$= P < 0.001,$****$ = P < 0.0001 (unpaired Student's t-test). Images shown are representative of three independent repeats.

FIG S1. Neutralization of the WA.1, B.1.617.2 and BA.1 pseudoviruses with nine serum samples collected from the selected volunteers during 1st batch (early) (A) and second batch (late) (B) of sample collection. 100% neutralization is considered as obtained by the

Polyclonal SARS CoV-2 (NB100-56578) antibody. All data shown are averages of the results of at least three independent experiments ± SD.

Fig S2. (A) The binding profile of the selected serum samples to wild type RBD displayed on the yeast surface. (B-D) Histograms showing yeast cells binding to the indicated serum samples, were sorted into eight gates based upon low to high binding affinity and the frequency of each variant's barcode in individual gates was determined by Illumina sequencing.

Fig S3. Validation of the epitope mapping results was carried out by quantifying the binding of WT and the selected RBD mutants to BCRTH-01, INK09 and INK36 serum (A-C) Histograms showing binding of the yeast cells displaying WT or mutant RBDs to the indicated serum samples, sorted into gates based upon low to high binding. Each image is a representative of two independent experiments performed in triplicates.

FIG S4. Multiple sequence alignment of different sarbecovirus spike RBD sequences showing conservation of the Class5/ RBD epitope residues marked by black triangles.

FIG S5. Shortlisted 29 sera show neutralising activity against XBB. 1.5. Neutralisation curves for WA. 1 and XBB. 1.5 pseudoviruses with serial dilutions of all the 29 shortlisted sera as indicated.

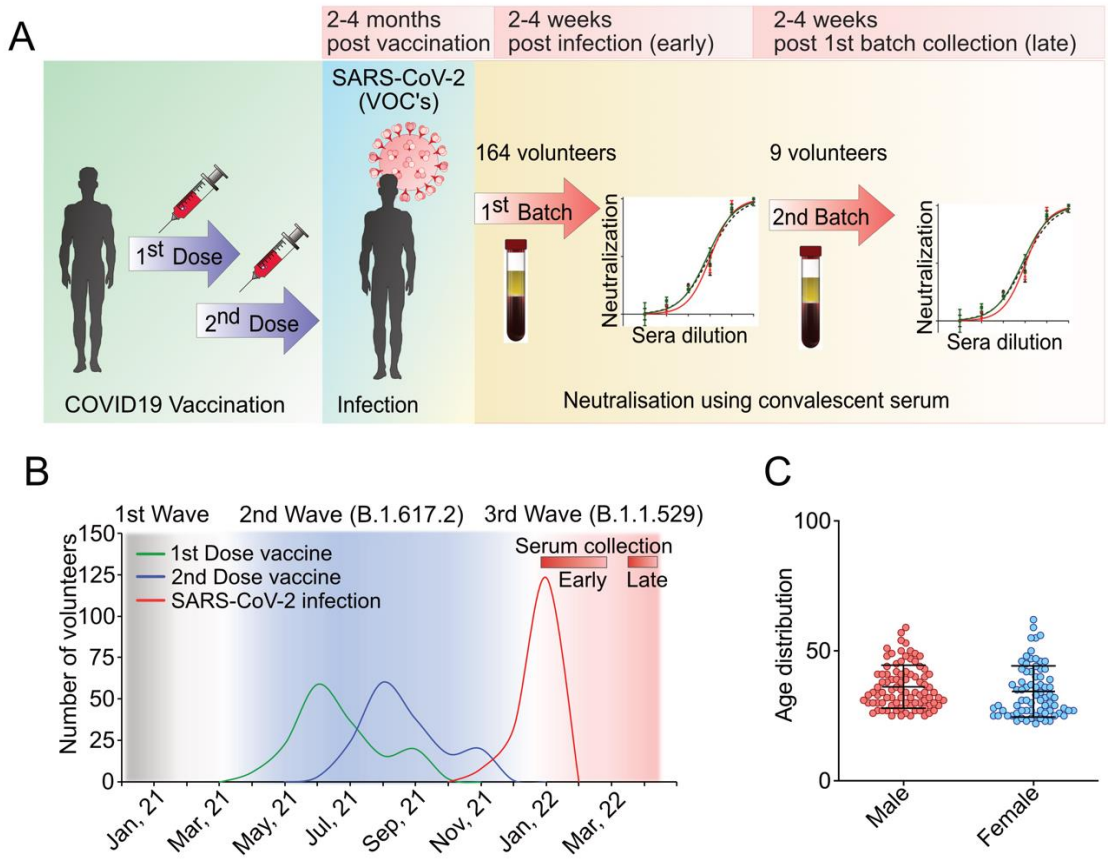
A
2-4 months
post vaccination
2-4 weeks
post infection (early)
2-4 weeks
post 1st batch collection (late)
SARS-CoV-2
(VOC's)
164 volunteers
9 volunteers
1st Dose
2nd Dose
1st Batch
2nd Batch
Neutralization
Sera dilution
COVID19 Vaccination
Infection
Neutralisation using convalescent serum
B
1st Wave
2nd Wave (B.1.617.2)
3rd Wave (B.1.1.529)
Serum collection
Early
Late
1st Dose vaccine
2nd Dose vaccine
SARS-CoV-2 infection
Number of volunteers
150
125
100
75
50
25
0
Jan, 21
Mar, 21
May, 21
Jul, 21
Sep, 21
Nov, 21
Jan, 22
Mar, 22
C
Age distribution
100
50
0
Male
Female

FIG.1

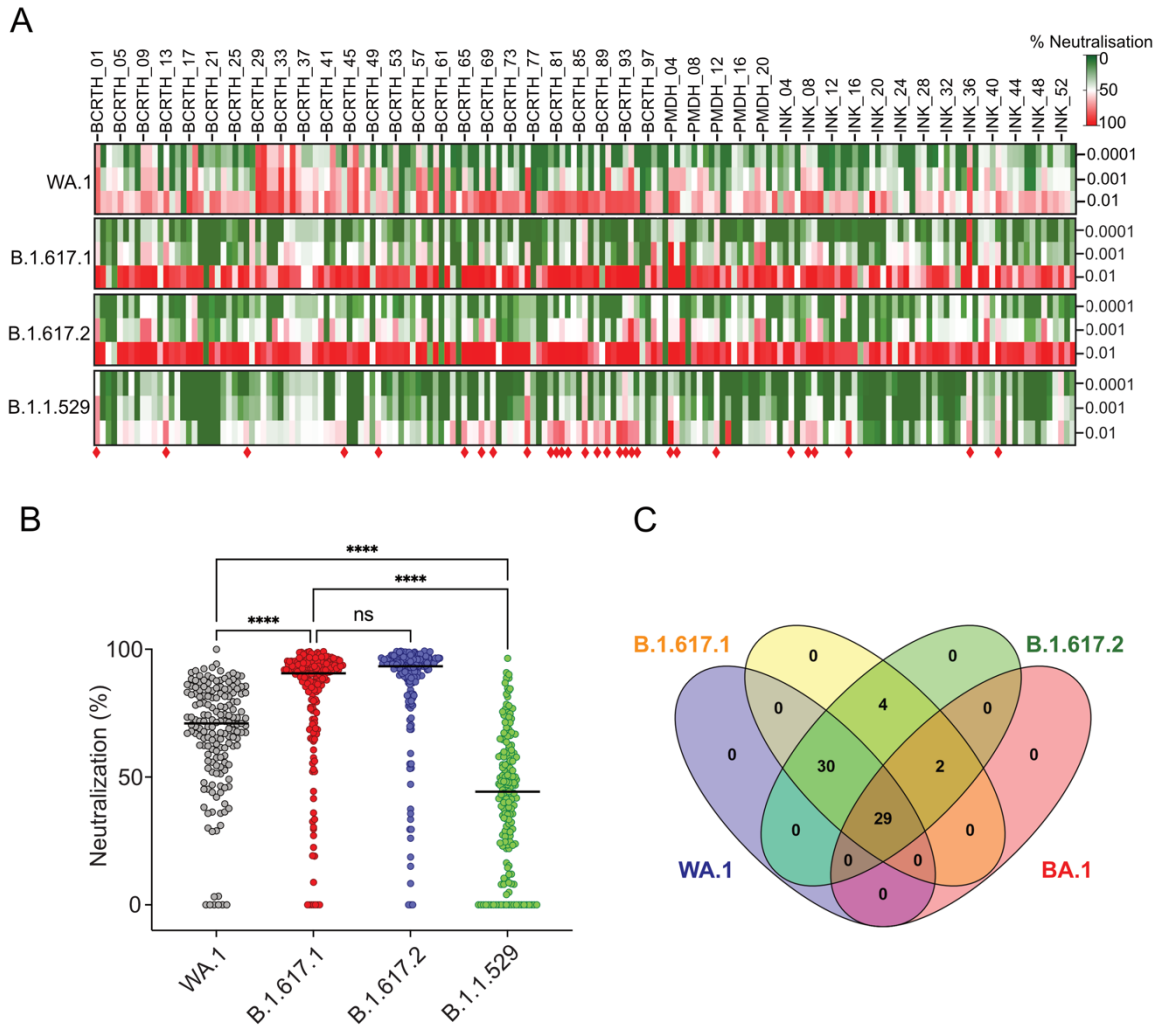

1248

1249 **FIG 2.**

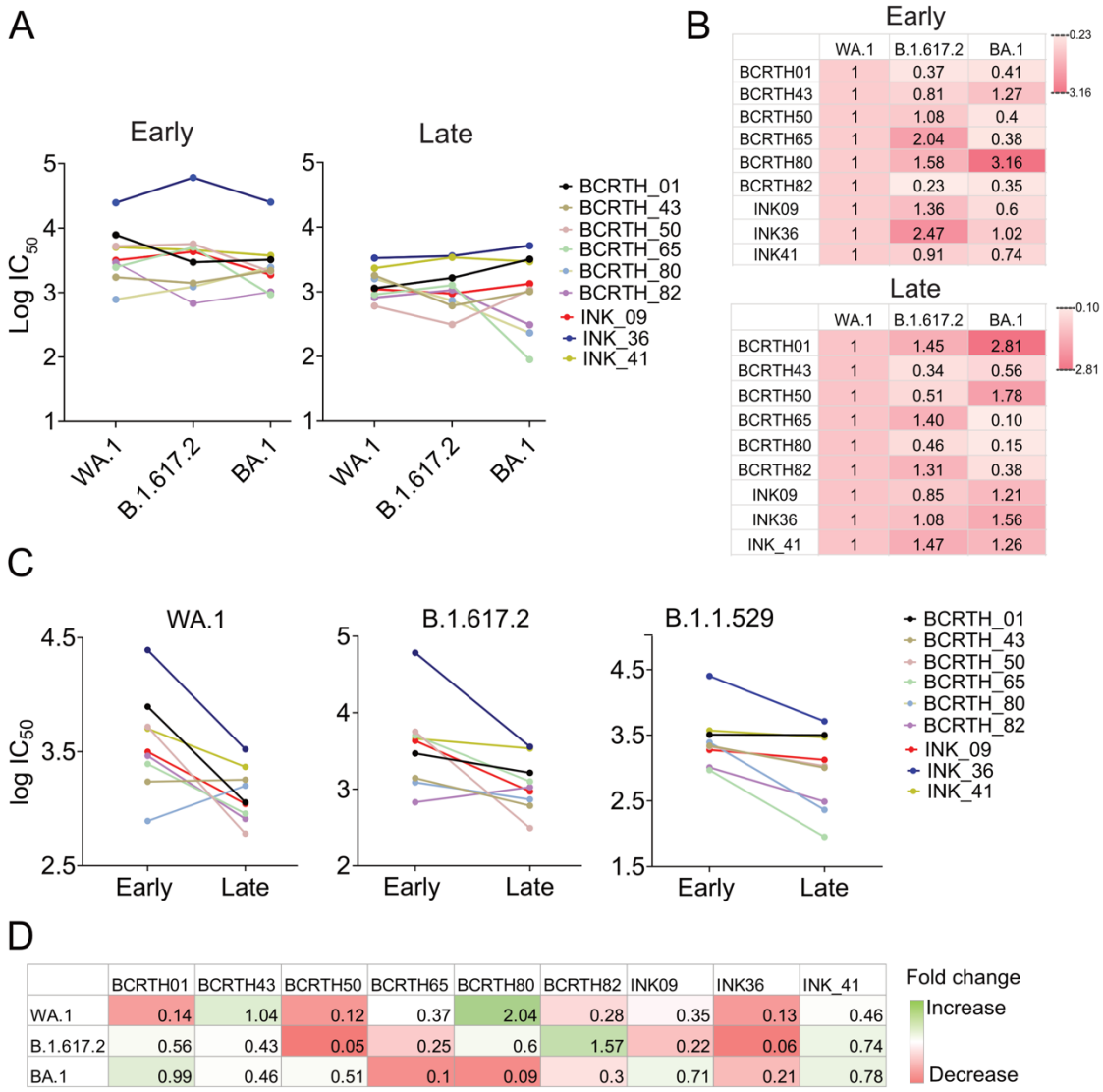

	WA.1	B.1.617.2	BA.1
BCRTH01	1	0.37	0.41
BCRTH43	1	0.81	1.27
BCRTH50	1	1.08	0.4
BCRTH65	1	2.04	0.38
BCRTH80	1	1.58	3.16
BCRTH82	1	0.23	0.35
INK09	1	1.36	0.6
INK36	1	2.47	1.02
INK41	1	0.91	0.74

	WA.1	B.1.617.2	BA.1
BCRTH01	1	1.45	2.81
BCRTH43	1	0.34	0.56
BCRTH50	1	0.51	1.78
BCRTH65	1	1.40	0.10
BCRTH80	1	0.46	0.15
BCRTH82	1	1.31	0.38
INK09	1	0.85	1.21
INK36	1	1.08	1.56
INK_41	1	1.47	1.26

	BCRTH01	BCRTH43	BCRTH50	BCRTH65	BCRTH80	BCRTH82	INK09	INK36	INK_41
WA.1	0.14	1.04	0.12	0.37	2.04	0.28	0.35	0.13	0.46
B.1.617.2	0.56	0.43	0.05	0.25	0.6	1.57	0.22	0.06	0.74
BA.1	0.99	0.46	0.51	0.1	0.09	0.3	0.71	0.21	0.78

FIG 3.

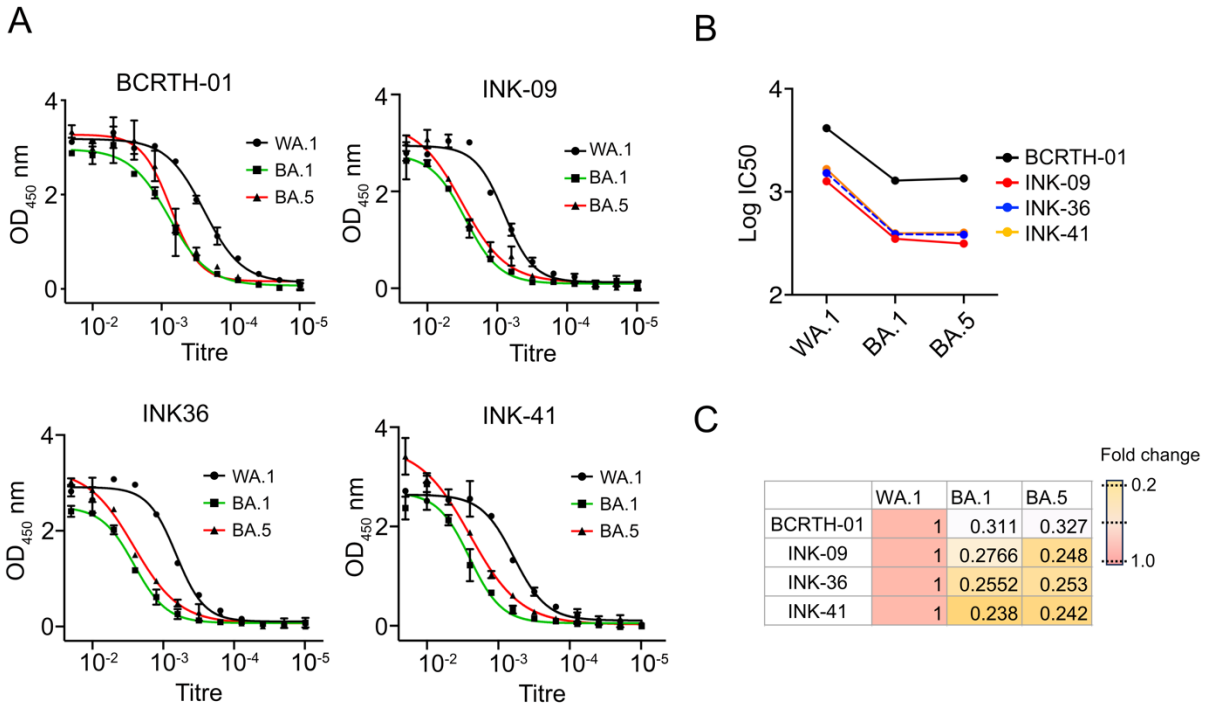

	WA.1	BA.1	BA.5
BCRTH-01	1	0.311	0.327
INK-09	1	0.2766	0.248
INK-36	1	0.2552	0.253
INK-41	1	0.238	0.242

FIG 4.

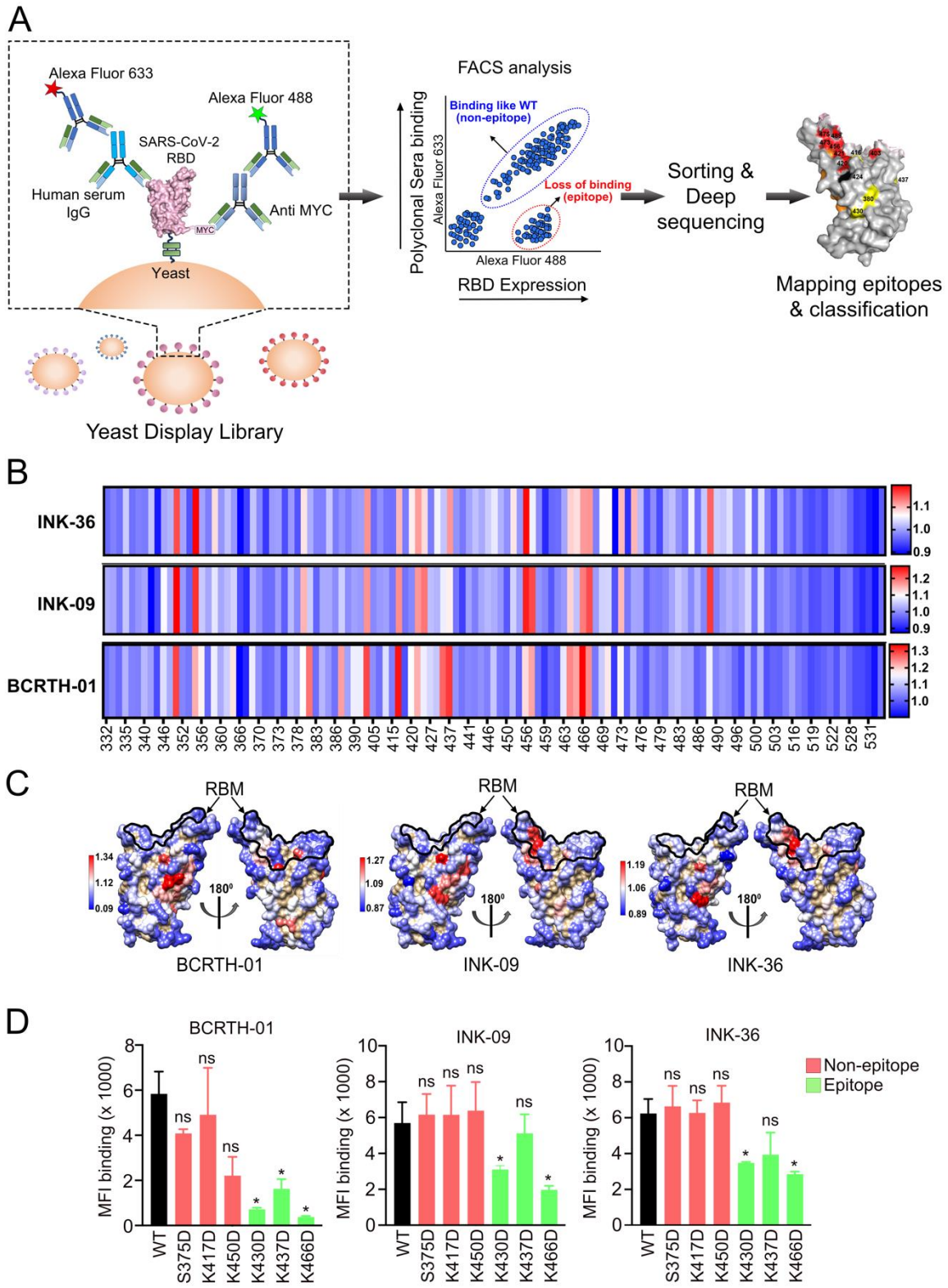
A
Alexa Fluor 633
Alexa Fluor 488
SARS-CoV-2 RBD
Human serum IgG
Anti MYC
MYC
Yeast
Yeast Display Library
FACS analysis
Polyclonal Sera binding
Alexa Fluor 633
Binding like WT (non-epitope)
Loss of binding (epitope)
Alexa Fluor 488
RBD Expression
Sorting & Deep sequencing
Mapping epitopes & classification
B
INK-36
INK-09
BCRTH-01
C
RBM
180°
BCRTH-01
INK-09
INK-36
D
BCRTH-01
INK-09
INK-36
MFI binding (x 1000)
Non-epitope
Epitope
WT
S375D
K417D
K450D
K430D
K437D
K466D
ns
*

FIG 5.

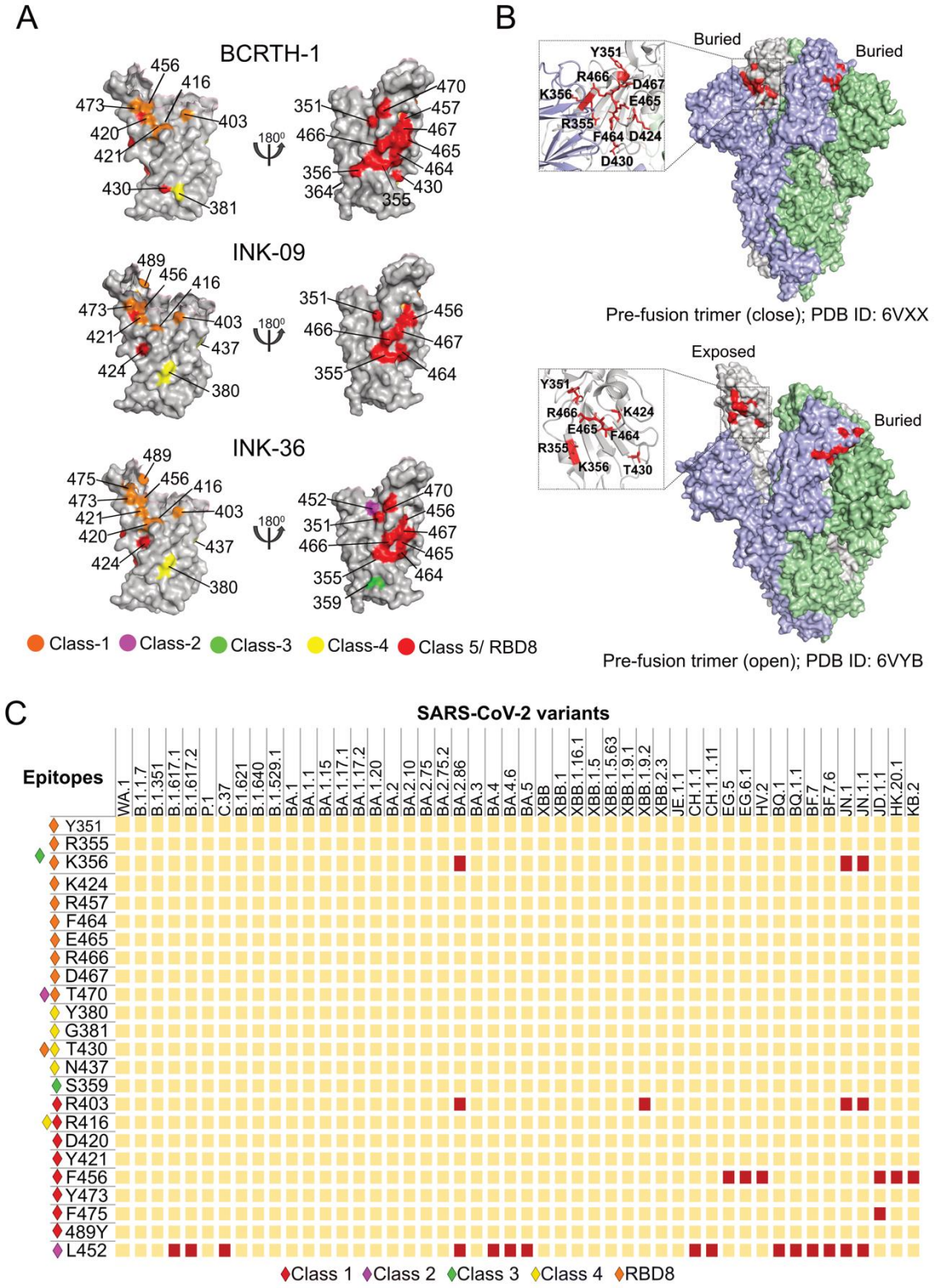
A
BCRTH-1
456
416
473
403
420
421
430
381
180°
351
470
457
466
467
465
356
464
364
430
355
INK-09
489
456
416
473
403
421
437
424
380
180°
351
456
466
467
355
464
INK-36
489
475
456
416
473
403
421
420
437
424
380
180°
452
470
456
351
467
466
465
355
464
359
Class-1
Class-2
Class-3
Class-4
Class 5/ RBD8
B
Buried
Buried
Y351
R466
D467
K356
E465
R355
F464
D424
D430
Pre-fusion trimer (close); PDB ID: 6VXX
Exposed
Buried
Y351
R466
K424
E465
F464
R355
K356
T430
Pre-fusion trimer (open); PDB ID: 6VYB
C
SARS-CoV-2 variants
Epitopes
WA.1
B.1.1.7
B.1.351
B.1.617.1
B.1.617.2
P.1
C.37
B.1.621
B.1.640
B.1.529.1
BA.1
BA.1.1
BA.1.15
BA.1.17.1
BA.1.17.2
BA.1.20
BA.2
BA.2.10
BA.2.75
BA.2.75.2
BA.2.86
BA.3
BA.4
BA.4.6
BA.5
XBB
XBB.1
XBB.1.16.1
XBB.1.5
XBB.1.5.63
XBB.1.9.1
XBB.1.9.2
XBB.2.3
JE.1.1
CH.1.1
CH.1.1.11
EG.5
EG.6.1
HV.2
BQ.1
BQ.1.1
BF.7
BF.7.6
JN.1
JN.1.1
JD.1.1
HK.20.1
KB.2
Y351
R355
K356
K424
R457
F464
E465
R466
D467
T470
Y380
G381
T430
N437
S359
R403
R416
D420
Y421
F456
Y473
F475
489Y
L452
Class 1
Class 2
Class 3
Class 4
RBD8

FIG 6.

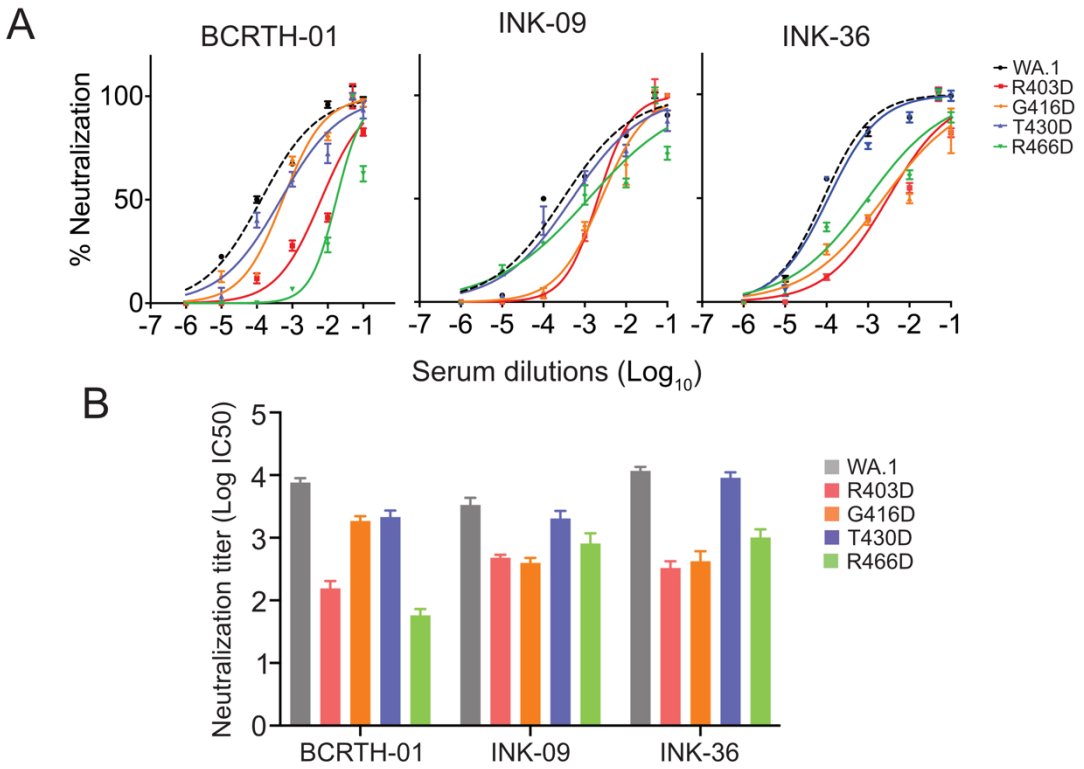

1265
1266 **FIG 7.**
1267

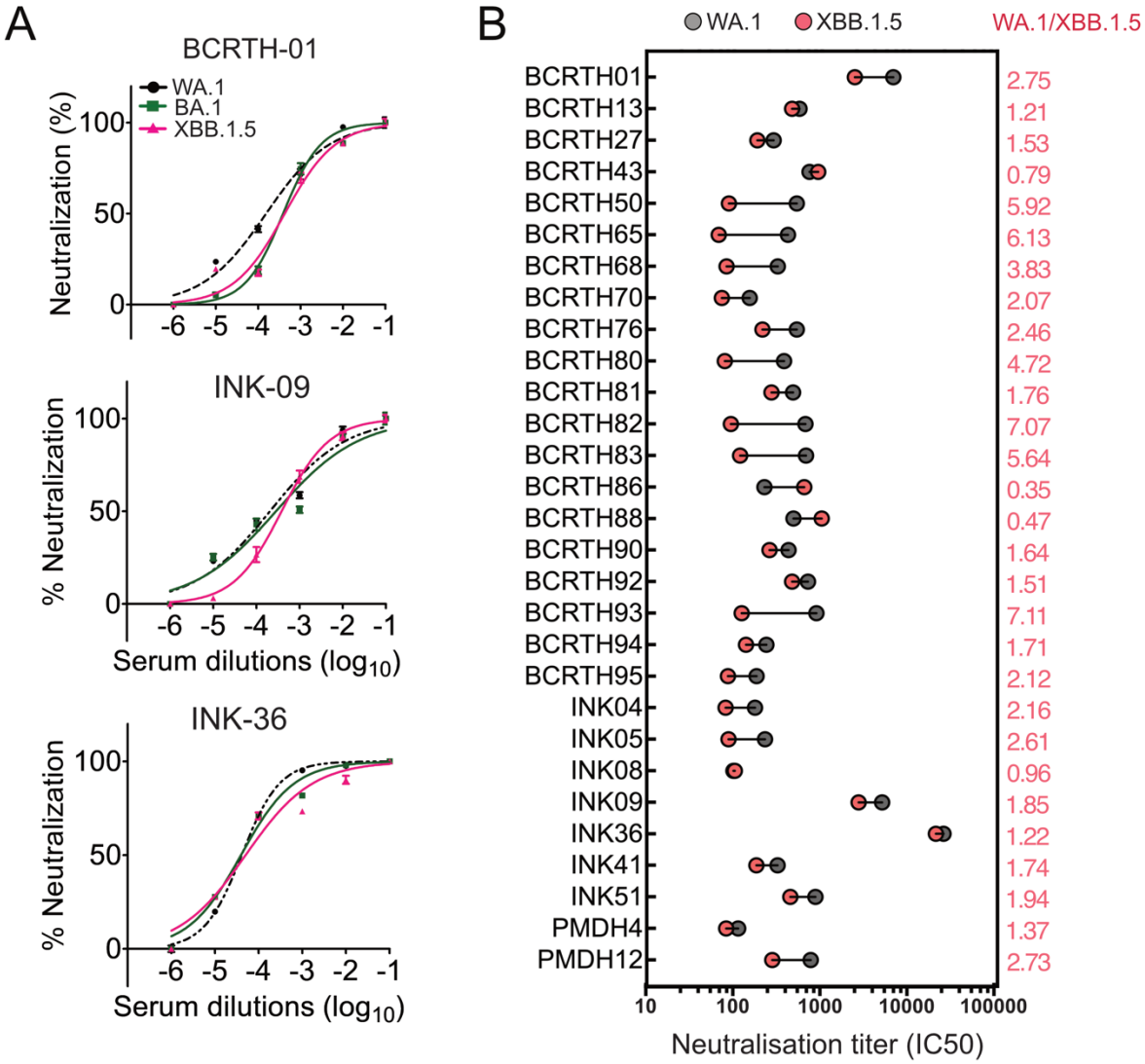
A
BCRTH-01
WA.1
BA.1
XBB.1.5
Neutralization (%)
100
50
0
-6 -5 -4 -3 -2 -1
INK-09
% Neutralization
Serum dilutions (log10)
INK-36
B
WA.1
XBB.1.5
WA.1/XBB.1.5
BCRTH01 2.75
BCRTH13 1.21
BCRTH27 1.53
BCRTH43 0.79
BCRTH50 5.92
BCRTH65 6.13
BCRTH68 3.83
BCRTH70 2.07
BCRTH76 2.46
BCRTH80 4.72
BCRTH81 1.76
BCRTH82 7.07
BCRTH83 5.64
BCRTH86 0.35
BCRTH88 0.47
BCRTH90 1.64
BCRTH92 1.51
BCRTH93 7.11
BCRTH94 1.71
BCRTH95 2.12
INK04 2.16
INK05 2.61
INK08 0.96
INK09 1.85
INK36 1.22
INK41 1.74
INK51 1.94
PMDH4 1.37
PMDH12 2.73
10 100 1000 10000 100000
Neutralisation titer (IC50)

FIG 8.

Acknowledgement:

This study is supported by the Indian Council for Medical Research (VIR/COVID-19/19/2021/ECD-I) awarded to AM. A.M. acknowledges additional funding support from the Anusandhan National Research Foundation (SERB-DST (CRG/2022/003628). R.V. is a JC Bose Fellow of DST. This work was funded by a grant from the Bill and Melinda Gates Foundation (INV-042471) to RV. Funding for infrastructural support was from DST FIST, MHRD, and the DBT IISc Partnership Program. I.D.J. acknowledges the Science and Engineering Research Board (SERB) for the National Post Doctoral Fellowship (PDF/2023/000284) awarded to her. K.K. acknowledges the support of an MHRD-IISc doctoral fellowship. The authors acknowledge project staff Shyamal Manna for his support in blood collection. The funders had no role in study design, data collection and interpretation, or the decision to submit the work for publication.